AD_____
(Leave blank)

Award Number: W81XWH-08-1-0751

TITLE:

Identification of the Microtubule Inhibitor-Activated Bcl-xL Kinase: A Regulator of Breast Cancer Cell Chemosensitivity to Taxol

PRINCIPAL INVESTIGATOR: David Terrano

CONTRACTING ORGANIZATION: University of Arkansas for Medical Sciences,
Little Rock, AR 72205

REPORT DATE: ...October 2010

TYPE OF REPORT: Annual Summary

PREPARED FOR:
U.S. Army Medical Research and Materiel Command Fort Detrick, Maryland 21702-5012

DISTRIBUTION STATEMENT: (Check one)

□X Approved for public release; distribution unlimited

The views, opinions and/or findings contained in this report are those of the author(s) and should not be construed as an official Department of the Army position, policy or decision unless so designated by other documentation.

REPORT DOCUMENTATION PAGE

Form Approved
OMB No. 0704-0188

Public reporting burden for this collection of information is estimated to average 1 hour per response, including the time for reviewing instructions, searching existing data sources, gathering and maintaining the data needed, and completing and reviewing this collection of information. Send comments regarding this burden estimate or any other aspect of this collection of information, including suggestions for reducing this burden to Department of Defense, Washington Headquarters Services, Directorate for Information Operations and Reports (0704-0188), 1215 Jefferson Davis Highway, Suite 1204, Arlington, VA 22202-4302. Respondents should be aware that notwithstanding any other provision of law, no person shall be subject to any penalty for failing to comply with a collection of information if it does not display a currently valid OMB control number. **PLEASE DO NOT RETURN YOUR FORM TO THE ABOVE ADDRESS.**

1. REPORT DATE *(DD-MM-YYYY)*	**2. REPORT TYPE**	**3. DATES COVERED** *(From - To)*
31-OCT-2010	Annual Summary	01 Oct 2009 - 30 Sep 2010

4. TITLE AND SUBTITLE
Identification of the Microtubule Inhibitor-Activated Bcl-xL Kinase: A Regulator of Breast Cancer Cell Chemosensitivity to Taxol

5a. CONTRACT NUMBER
W81XWH-08-1-0751

5b. GRANT NUMBER
BC083287

5c. PROGRAM ELEMENT NUMBER

6. AUTHOR(S)
David Terrano

Email: terranodavidt@uams.edu

5d. PROJECT NUMBER

5e. TASK NUMBER

5f. WORK UNIT NUMBER

7. PERFORMING ORGANIZATION NAME(S) AND ADDRESS(ES)
University of Arkansas for Medical Sciences,

Little Rock, AR 72205

8. PERFORMING ORGANIZATION REPORT NUMBER

9. SPONSORING / MONITORING AGENCY NAME(S) AND ADDRESS(ES)
U.S. Army Medical Research and Materiel Command
Fort Detrick, Maryland 21702-5012

10. SPONSOR/MONITOR'S ACRONYM(S)

11. SPONSOR/MONITOR'S REPORT NUMBER(S)

12. DISTRIBUTION / AVAILABILITY STATEMENT
Approved for public release; distribution unlimited

13. SUPPLEMENTARY NOTES

14. ABSTRACT

This training grant set out to define a molecular pathway involved in breast tumor resistance to the key chemotherapeutic class of drugs called microtubule inhibitors (MTIs). It is also designed to train the Principal Investigator (PI) as a future breast cancer physician-scientist. MTIs are the most actively used agents for metastatic and adjuvant BC therapy, yet their use is limited by resistance and side effects. They activate a kinase that phosphorylates and inactivates Bcl-xL, an anti-apoptotic protein that causes resistance to chemotherapeutic agents. The goal is to identify the Bcl-xL kinase first by developing an *in vitro* assay for it. Previously, we showed that Cdk1/cyclin B1, the master mitotic kinase, phosphorylates Bcl-xL *in vitro*. Studies here confirm that it also phosphorylates Bcl-xL in cells not only following MTI treatment but also during normal mitosis. Furthermore, preliminary data indicate that Bcl-xL phosphorylation increases tumor cell apoptosis. From there, a clinical research study is underway to study Bcl-xL phosphorylation in patients who have breast cancer and are treated with MTIs.

15. SUBJECT TERMS
Microtubule inhibitors, breast cancer, Bcl-xL, vinblastine, Cdk1, cyclin B, mitotic arrest

16. SECURITY CLASSIFICATION OF:			**17. LIMITATION OF ABSTRACT**	**18. NUMBER OF PAGES**	**19a. NAME OF RESPONSIBLE PERSON**
a. REPORT	**b. ABSTRACT**	**c. THIS PAGE**			USAMRMC
U	U	U	UU	62	**19b. TELEPHONE NUMBER** *(include area code)*

Table of Contents

Page

Introduction……..…….1

Body……...2

Key Research Accomplishments……...4

Reportable Outcomes……4

Conclusion……5

References……5

Appendices……...7

INTRODUCTION: This training grant set out to identify and characterize the Bcl-xL kinase as a potential factor in resistance to actively used chemotherapeutics, microtubule inhibitors (MTIs) and, to train the Principal Investigator (PI) as a future breast cancer physician-scientist. MTIs are the most actively used agents for metastatic and adjuvant BC therapy, yet their use is limited by resistance and side effects (1-4). Bcl-xL is an anti-apoptotic protein that causes resistance to chemotherapeutic agents when overexpressed in many tumor types. Following MTI treatment, Bcl-xL is phosphorylated and inactivated (4) possibly representing a molecular pathway that leads to resistance when inactivated. The initial scientific aims, developing a Bcl-xL kinase and identifying the kinase *in vitro* as Cdk1/cyclin B1, were reported in 2009. This report outlines experiments showing that Cdk1/cyclin B1 phosphorylated Bcl-xL in cultured KB-3 cells and partially sensitized them cells to MTIs. The latter data shifted us toward the ultimate goal, which is investigating the correlation between Bcl-xL kinase activity, Bcl-xL phosphorylation, and breast tumor cell sensitivity to MTIs.

The specific breast cancer training plan was designed to educate the PI as follows. 1) Understand the molecular biology behind tumor cell death following treatment with anti-cancer agents; 2) Translate that work

into clinical studies (an actual clinical protocol and a survey study outlined below); 3) Learn the clinical side of breast cancer, through clinical and inpatient medical school education; and 4) Learning collaboration and communication skills with both clinical and basic science breast cancer researchers through a monthly Breast Cancer Focus Group (designed by the PI), research seminars, dissertation writing, publication, and presentations at professional meetings and departmental seminars.

BODY:

Laboratory data

The last annual update reported that Cdk1/cyclin B1 was the MTI-activated Bcl-xL kinase *in vitro*. We also discovered that Bcl-xL was partially phosphorylated during normal mitosis, a novel finding to date. Since then, experiments confirmed our *in vitro* assay studies and were validated in cell culture studies using Cdk inhibitors. These data comprised our publication in the Molecular and Cellular Biology Journal, available on PubMed and the Molecular and Cellular Biology Journal. The Word document that was converted to a PDF of the publication now is in the "APPENDICES" section. Highlighted data figures from that publication and that support the text here are also in the "APPENDICES", specifically "APPENDIX 1."

Previously, we developed a 12 amino acid peptide harboring the MTI-induced phosphorylation site Ser62 in Bcl-xL termed FL62. FL62 was highly phosphorylated by Cdk1/cyclin B1 partially purified from mitotic and MTI-treated KB-3 cells. In addition, we also reported that purified, activated Cdk1/cyclin A2 phosphorylated a full-length Bcl-xL substrate on Ser62, the known phosphorylation site (4). Since then we analyzed JNK as the Bcl-xL kinase, as previously reported. FL62 was not phosphorylated by gel-filtration elution fractions which contained JNK isoenzymes 1 and 2 (Fig. 1). Furthermore, when vinblastine treated KB-3 cells were depleted of Cdk1 using the Cdk1 binding protein Cks-1, FL62 phosphorylation decreased by an amount corresponding to depleted Cdk1/cyclin B1 without any change in JNK1 (data shown in previous report). This essentially argues against JNK as the Bcl-xL kinase.

To determine if Cdk1/cyclin B1 was the cellular Bcl-xL kinase, we conducted studies in KB-3 cells using three validated Cdk inhibitors, including roscovitine (ROS), purvalanol A (PA), and RO-3306 (RO) (5-7). The experiments were designed so that the inhibitors would not block or delay progression to mitosis. Cells were synchronized by double thymidine block, treated with vinblastine 1 h following release, and then treated with each Cdk inhibitor or dimethyl sulfoxide (DMSO) vehicle for 2 h at time points corresponding to G2 and M phases in KB-3 cells (Fig. 2A shows schematic). The 10 h, 11 h, and 12 h time points were thus chosen, where the 12 h time point represents a negative control because at this time point cells are already fully within mitosis and Bcl-xL is already phosphorylated (4). Indeed, this is likely the reason Cdk1/cyclin B1 was previously dismissed as the kinase (4). Fig. 2B shows that Ros inhibited any further increased of vinblastine induced Bcl-xL phosphorylation during the 10-12 h and 11-13 h time intervals. PA and RO, in contrast, reversed it probably by causing mitotic slippage since they are known to be more potent inhibitors than Ros (5-7). Slippage is shown by loss of phospho-H3 histone, a marker of mitosis. As expected, however, Bcl-xL phosphorylation was similar to the DMSO control from 12-14 h after adding Ros while PA and RO again reversed Bcl-xL phosphorylation. To prove that PA and RO caused mitotic slippage, we co-treated cells with the proteasome inhibitor MG132, preventing cyclin B1 degradation, which is the signal for mitotic exit. The results with Ros inhibition did not change. However, with PA and RO, adding MG132 maintained cyclin B1 and phospho-H3 histone levels. In turn, Bcl-xL phosphorylation was not reversed but inhibited from increasing (Fig. 2C). We then reasoned to use a 10-fold lower concentration of PA and RO (1 μM) because the initial experiments at 10 μM are 300- and 500-fold greater, respectively, than their *in vitro* IC50s for CDK1 (33 and 20 nM, respectively). That for Ros, however, was only 30-fold higher than its IC50 for CDK1 (650 nM) (5-7). Thus, to inhibit Cdk1 without causing mitotic slippage, 1 μM PA and RO each was used. This concentration of PA and RO prevented any further phosphorylation of Bcl-xL during the 11-13 h interval while maintaining cyclin B1 and phospho-H3 histone levels indicating that the cells did not exit mitosis (Fig. 2D).

The Cdk inhibitors are highly specific for Cdk1 and not other kinases *in vitro*, but could non-specifically inhibit other kinases, including other Cdks. Though our synchronization design attempts to avoid this, we addressed further. Thus, wild-type and Cdk2 knockout mouse fibroblasts were treated with vinblastine and phosphorylation was analyzed. There was partial Bcl-xL phosphorylation in both wild-type and Cdk2 knockout cells that was also equal (Fig. 3A), ruling out Cdk2 as the Bcl-xL kinase and an unlikely target of the Cdk inhibitors when added during mitosis. We also tested another mitotic kinase, Aurora B kinase, which is involved in the spindle assembly checkpoint that prevents anaphase before proper bipolar spindle attachment to chromosomes. Since it normally phosphorylates H3-histone, phosph-H3 histone was used as a marker for inhibition (8) while cyclin B1 and H1-histone phosphorylation levels were our markers for mitosis. Fig. 3B

shows that adding the Aurora B inhibitor ZM 44379 to vinblastine treated cells during mitosis reduced phospho-H3 histone levels almost completely without affecting Bcl-xL and Bcl-2 phosphorylation. Cyclin B1 and phospho-H1 histone levels were maintained signaling that cells remained in mitosis.

The data above strongly support Cdk1/cyclin B1 as the Bcl-xL kinase. This was then studied during normal mitosis where Cdk inhibitors were added to untreated synchronized mitotic cells. Bcl-xL and Bcl-2 phosphorylation were prevented by all three inhibitors but not by vehicle (Fig. 4). Also, cyclin B1 and phosho-H3 histone levels were unaffected indicating that the cells entered mitosis. We then hypothesized that if Cdk1/cyclin B1 phosphorylates Bcl-xL normally, then prolonging mitosis and hence Cdk1/cyclin B1 activity should lead to complete phosphorylation. Towards this end, the proteasome inhibitor MG132 was added to untreated mitotic cells. MG132 prolonged mitosis by increasing cyclin B1 levels and Cdk1/cyclin B1 activity (i.e. increased phospho-H1 histone levels Fig. 4B). Also, Bcl-xL and Bcl-2 phosphorylation went to maximal levels (Fig. 4B). In contrast, cells treated with vehicle showed dephosphorylation of Bcl-xL and Bcl-2 and loss of mitotic markers, indicating normal cell division.

The next step was to determine if Cdk1/cyclin B1 localized to the mitochondria, the primary location of Bcl-xL and Bcl-2. This was specific aim 2 of the original proposal. First, we showed that FL62 was only phosphorylated *in vitro* by mitochondria purified from vinblastine treated cells not from untreated cells (Fig. 5). Immunofluorescence studies then revealed a diffuse Cdk1 and cyclin B1 staining pattern that was coincident mitochondrial marker in vinblastine treated not control cells (see attached paper Figs. 10D and 10E in "APPENDIX 2" for high resolution of the data).

Lastly, we analyzed the role of Bcl-xL phosphorylation in Cdk1/cyclin B1 pro-apoptotics signaling, a controversial issue regarding Cdk1 function (11-13). KB-3 cells were transfected with wild-type or non-degradable cyclin B1 (cyclin B1 (R42A)-GFP) to show that prolonged Cdk1 activity leads to apoptosis. Non-degradable cyclin B1 induced significantly more apoptosis than GFP transfectants. Wild-type cyclin B1 did as well, but significantly less (Fig. 6A). Next KB-3 cells were co-transfected with non-degradable cyclin B1 and either wild-type, phospho-defective (S62A), or a phospho-mimic (S62D) mutant of Bcl-xL. Transfection with S62A Bcl-xL significantly blocked apoptosis induced by non-degradable cyclin B1 ($P \leq 0.001$ compared to wild-type Bcl-xL), while S62D did not ($P \leq 0.442$ compared to wild-type Bcl-xL) (Fig. 6B). Apoptosis protection was also not due to different expression levels (data not shown).

Translational research study

We continued the clinical protocol entitled "Alterations in the Bcl-2 Family Proteins in the Peripheral Blood Following Treatment with Taxanes in Patients with Breast Cancer." The study was approved by the UAMS Institutional Review Board (IRB) in 2009. The goal is to determine if Bcl-xL, Bcl-2, and Mcl-1 are phosphorylated in peripheral blood mononuclear cells following taxane treatment. Then we will analyze if that phosphorylation correlates with a disease response or non-response, or with more or less side effects. Peripheral blood mononuclear cells will act as a surrogate marker if the hypothesis is affirmed. If it is not, then it can serve as an internal control when studying actual tumor samples.

The results from two patients who have breast cancer did not show Bcl-xL or Bcl-2 phosphorylation before or after taxane therapy. While Bcl-xL levels were absent in one sample after taxane therapy, it is unclear if it is due to a change in cell population. In addition, cyclin B1 levels did not increase, suggesting that the cells were not mitotically arrested. The reason may be that the cells obtained are already differentiated and thus post-mitotic, the cell population changes after treatment, or the number of mitotic cells is too low to detect any changes. More samples are needed to reproduce the initial data and increase the sample size. However, cell sorting and flow cytometry techniques can be employed to determine if mitotic cells are present and, if so, isolate them for analysis of Bcl-xL, Bcl-2, and Mcl-1phosphorylation.

Specific training tasks

My training proceeded as planned in the original proposal. Scientifically, my written dissertation was approved and successfully defended as stated in the 2009 report. I continue to collaborate and conduct experiments, including the translational study above. Dr. Chambers and I were invited to write a review for the journal Cell Division discussing mitosis, mitotic arrest, and apoptosis. The manuscript is currently in preparation. For career development, I presented a poster at the American Society for Clinical Investigation/American Physician Scientists Association and the Central Society for Clinical Research annual meetings in April 2010, continued medical school rotations (several within the oncology), and continued to organizing the UAMS Breast Cancer Focus Group.

In a new and exciting development, I will conduct clinical research study that is unrelated to the current project but related to breast cancer. It is explores the social side of breast cancer. The study is entitled "Understanding of Bio-Banking in African American Patients who have Cancer Understanding of Bio-Banking in African American Patients who have Cancer." The proposal asks if African American (AA) patients who have breast cancer understand bio-banking and if that influences their decision to donate. The study will be part of the Biospecimen Management Program (**BMaP**) study at UAMS. The **BMaP** study is funded by the Cancer Research Network at the NCI directed at UAMS by breast surgical oncologist Ronda Henry-Tillman, M.D. **BMaP** is a multi-center study that aims improve the quality and quantity of biological specimens collected from AA and minority populations who have cancer in the mid-south region. Currently, AAs donate their tissues for research at lower rates than Caucasian (13) populations and they also express less trust of physicians (14). Patients will be asked about their understanding of tissue donation for research, and then educated about it afterwards. Differences between racial populations will be compared. I attended a regional **BMaP** planning meeting in June 2010 at Meharry Medical College in Nashville, Tennessee where my study garnered significant interest. The study came about when applying for the Bruce and Brandon Lee scholarship in the UAMS Medical Humanities department. The scholarship is dedicated to better understanding ethical and social issues involved of oncology. Students can propose any idea they wish, and only one is offered a scholarship. To find a proposal, I sought out Dr. Henry-Tillman after one of her administrators presented their work at a Breast Cancer Focus Group meeting. There, she suggested this idea, which I then independently researched. I was fortunate to be offered that one scholarship. Currently, IRB approval is underway. It was a great learning experience in collaboration and will be an interesting study.

KEY RESEARCH ACCOMPLISHMENTS:

Basic Research

- FL62 kinase is distinct from JNK.
- Cdk inhibitors inhibit vinblastine-induced Bcl-xL/Bcl-2 phosphorylation.
- Inhibition of Bcl-xL/Bcl-2 phosphorylation is not a consequence of mitotic slippage.
- Vinblastine induces Bcl-xL phosphorylation in Cdk2-null cells.
- Inhibition of aurora B does not affect vinblastine-induced Bcl-xL/Bcl-2 phosphorylation.
- Cdk-dependent mitotic Bcl-xL/Bcl-2 phosphorylation.
- Prolongation of mitosis in the absence of microtubule inhibition is sufficient to induce extensive Bcl-xL/Bcl-2 phosphorylation.
- Mitochondrial localization of Cdk1/cyclin B.
- Phosphodefective Bcl-xL blocks cell death induced by non-degradable cyclin B1.

Clinical Research

- Co-author of the clinical research protocol "Alterations in the Bcl-2 Family Proteins in the Peripheral Blood Following Treatment with Taxanes in Patients with Breast Cancer." Accepted by the UAMS Institutional Review Board **(Study protocol #109857).**
- Bruce and Brandon Lee Scholarship, UAMS Department of Humanities. Advisors: Chris Hackler, PhD and Rhonda Henry-Tillman, M.D.
  - Title: Understanding of Bio-Banking in African American Patients who have Cancer (IRB pending).

REPORTABLE OUTCOMES:

Publications, Posters, and Presentations

- **Terrano, D.T**. and Chambers T.C. Cyclin-Dependent Kinase 1-Mediated Bcl-xL/Bcl-2 Phosphorylation Acts as a Functional Link Coupling Mitotic Arrest and Apoptosis. Mol. Cell. Biol., 2010, 30(3), 640-656. PMID 19917720.
- **Terrano, D.T**. and Chambers T.C. Mitosis, Mitotic arrest, and Apoptosis in response to microtubule inhibitors, Cell Division, *Invited review* (Manuscript in preparation).
- **D Terrano**, JJ Joheim, N Sakurikar, I Makhoul, LF Hutchins and TC Chambers. CDK1/Cyclin B1 Mediate Bcl-xL/Bcl-2 Phosphorylation is a Pro-Apoptotic Signal Following Mitotic Arrest and Microtubule Inhibitor

Treatment. Abstract Number 79. The American Society of Clinical Investigation/American Association of Physician Scientists Joint Meeting, 2010, Chicago, IL.

- **D Terrano**, JJ Joheim, N Sakurikar, I Makhoul, LF Hutchins and TC Chambers. CDK1/Cyclin B1 Mediate Bcl-xL/Bcl-2 Phosphorylation is a Pro-Apoptotic Signal Following Mitotic Arrest and Microtubule Inhibitor Treatment. Poster 74. Central Society for Clinical Research and Midwestern Section American Federation for Medical Research Combined Annual Meeting, 2010, Chicago, IL.
- Renewal of Dr. Chambers' RO1, 2 R01 CA-109821-06, based on data from PI's work.
- Written dissertation: Identification of CDK1 as the Vinblastine Activated Bcl-xL Kinase.

Clinical Activities

- Surgical pathology clinical rotation as part of the MD training of his MD/PhD program.
- Co-author of ongoing clinical protocol #109857"Alterations in the Bcl-2 Family Proteins in the Peripheral Blood Following Treatment with Taxanes in Patients with Breast Cancer."
- Breast Cancer Focus Group at UAMS, monthly meetings.
- Bruce and Brandon Lee Scholarship, UAMS Department of Humanities. Advisors: Chris Hackler, PhD and Dr. Rhonda Henry-Tillman, M.D.
  - Title: Understanding of Bio-Banking in African American Patients who have Cancer.
  - IRB approval pending.

CONCLUSION: The data above strongly suggest that phosphorylation of Bcl-xL plays some role on Cdk1/cyclin B1 pro-apoptotic signaling. In fact, recent data show that Mcl-1 (14), an anti-apoptotic Bcl-2 family protein also phosphorylated following MTI treatment, is also a Cdk1/cyclin B1 substrate. More importantly, phosphorylation leads to proteasome degradation, a potential signal for cell death following prolonged mitosis. Together, these data suggest that Cdk1/cyclin B1 phosphorylation of these proteins may act as a sensor for the duration of mitosis where prolonged mitosis leads to maximal phosphorylation and inactivation of Bcl-xL, Bcl-2, and Mcl-1. In turn, cells are more sensitive to cell death signals perhaps by the pro-apoptotic Bcl-2 proteins which Bcl-xL, Bcl-2, and Mcl-1 directly inhibit. The cells then begin apoptotic signaling, exit mitosis, and die. While past and current data indicate Cdk1/cyclin B1 protects against mitosis by phosphorylation and inhibition of caspase-9 (11) and phosphorylation and stabilization of pro-survival protein survivin (12), the duration of mitosis was critical to this function in both studies. Experiments are underway to understand this and the link between Cdk1/cyclin B1 and apoptosis. In addition, the proposal continues to explores translational avenues that support the laboratory work and in a new public health study that trains the PI in breast cancer clinical research strategy, design, and implementation.

REFERENCES

1. Kummel, S, Krocker, J, Kohls, A, Breitbach, G-P, Morack, G, Budner, M et al (2006) Randomised trial: survival benefit and safety of adjuvant dose-dense chemotherapy for node-positive breast cancer. Brit J Cancer 11;94:1237-44.
2. McGrogan BT, Gilmartin B, Caney DN, McCann A. (2008) Taxanes, microtubules and chemoresistant breast cancer Bioch. Biophys Acta 1785(2):96-132.
3. Du,L., Lyle,C.S., and Chambers,T.C. (2005). Characterization of vinblastine-induced Bcl-xL and Bcl-2 phosphorylation: evidence for a novel protein kinase and a coordinated phosphorylation/dephosphorylation cycle associated with apoptosis induction. Oncogene *24*, 107-117.
4. Upreti,M., Galitovskaya,E.N., Chu,R., Tackett,A.J., Terrano,D.T., Granell,S., and Chambers,T.C. (2008). Identification of the Major Phosphorylation Site in Bcl-xL Induced by Microtubule Inhibitors and Analysis of Its Functional Significance. J. Biol. Chem. *283*, 35517-35525.
5. Inagaki, J. G. Delcros, and J. P. Moulinoux. 1997. Biochemical and cellular effects of roscovitine, a potent and selective inhibitor of the cyclin-dependent kinases cdc2, cdk2 and cdk5. Eur. J. Biochem. 243:527–536.
6. Rosania, G. R., J. Merlie, Jr., N. Gray, Y. T. Chang, P. G. Schultz, and R. Heald. 1999. A cyclin-dependent kinase inhibitor inducing cancer cell differentiation: biochemical identification using Xenopus egg extracts. Proc. Natl. Acad. Sci. U. S. A. 96:4797–4802.

7. Vassilev, L. T., C. Tovar, S. Chen, D. Knezevic, X. Zhao, H. Sun, D. C. Heimbrook, and L. Chen. 2006. Selective small-molecule inhibitor reveals critical mitotic functions of human CDK1. Proc. Natl. Acad. Sci. U. S. A. 103:10660–10665.
8. Hsu, J. Y., Z. W. Sun, X. Li, M. Reuben, K. Tatchell, D. K. Bishop, J. M. Grushcow, C. J. Brame, J. A. Caldwell, D. F. Hunt, R. Lin, M. M. Smith, and C. D. Allis. 2000. Mitotic phosphorylation of histone H3 is governed by Ipl1/aurora kinase and Glc7/PP1 phosphatase in budding yeast and nematodes. Cell 102:279-291.
9. Allan, L. A. and P. R. Clarke. 2007. Phosphorylation of caspase-9 by CDK1/cyclin B1 protects mitotic cells against apoptosis. Mol. Cell 26:301-310.
10. O'Connor, D. S., N. R. Wall, A. C. Porter, and D. C. Altieri. 2002. A p34(cdc2) survival checkpoint in cancer. Cancer Cell **2**:43-54.
11. Allan, L.A. and P.R. Clarke. 2009. Apoptosis and autophagy: Regulation of caspase-9 by phosphorylation. FEBS Journal 276: 6063-6073.
12. Harley, M.E, Allan, L.A., Sanderson, H.S., and Clarke, P.R. 2010. Phosphorylation of Mcl-1 by CDK1-cyclin B1 initiates its Cdc20 dependent destruction during mitotic arrest. EMBO Journal. 29: 2407-2420.
13. Wendler D, and Emanuel E. 2002 Research with stored biological samples: what do research participants want? Arch Intern Med 2002; 162:1457–62.
14. Hall MA, Camacho F, Lawlor JS, Depuy V, Sugarman J, Weinfurt K. 2006. Measuring trust in medical researchers. Med Care 2006;44: 1048–53.

APPENDIX 1: Data supporting text in “BODY” section above.

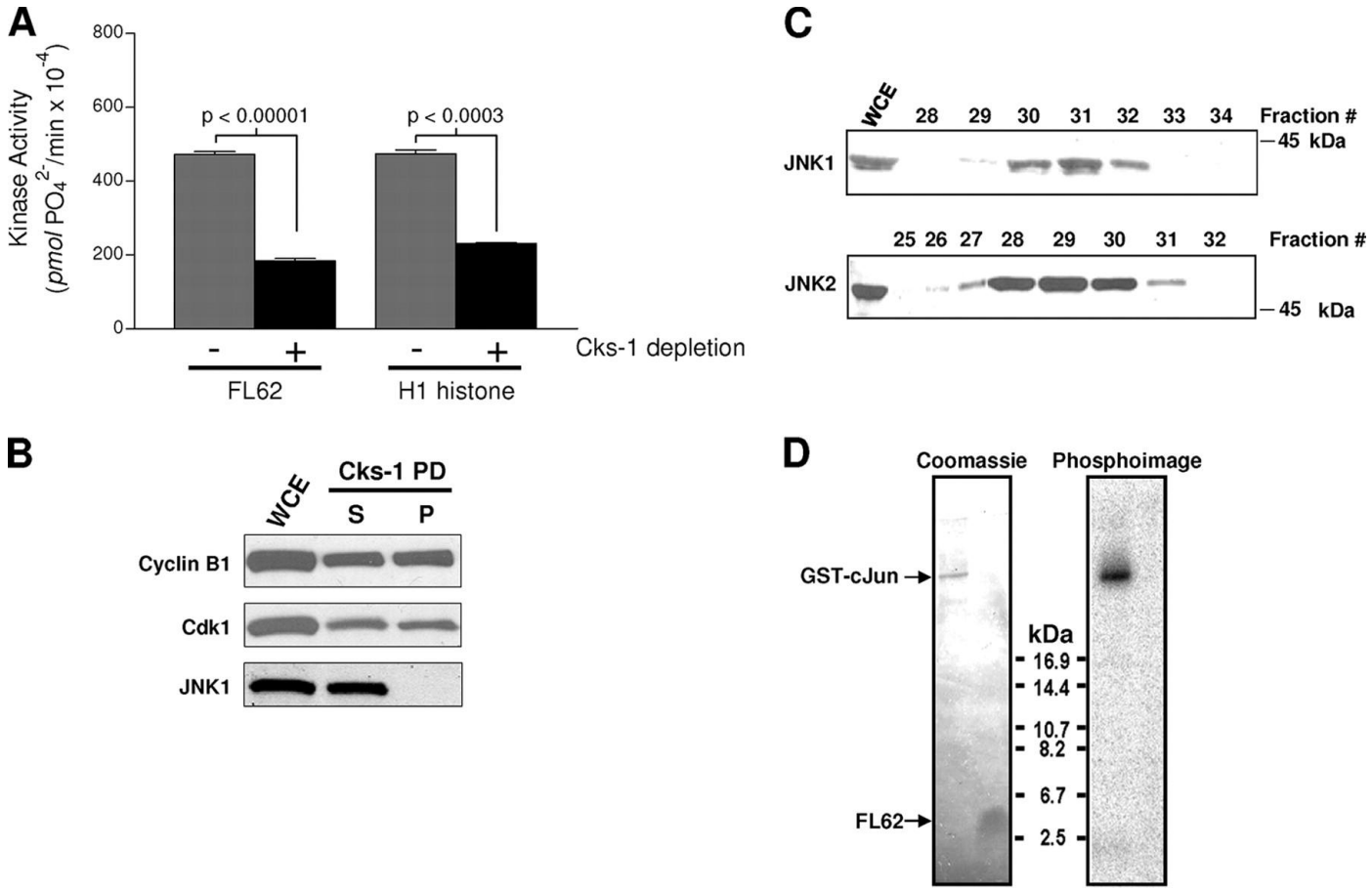

Fig. 1. FL62 kinase is a cyclin-dependent kinase and is distinct from JNK. A whole-cell extract (WCE) of KB-3 cells treated with vinblastine (30 nM, 16 h) was incubated with Cks-1-conjugated agarose beads. (A) The original extract and that depleted with Cks-1 were incubated with FL62(10 µg) or H1 histone (1 µg) for 20 min at 30°C in a kinase reaction mixture containing 10 µM ATP and 1 µCi [γ^{32}P]ATP, and phosphorylation was determined using the P81 filter paper assay. Phosphorylation in the absence of a substrate was subtracted. Data are means standard deviations (*n* = 3). (B) The WCE, as well as the supernatant (S) and the pellet (P) from the Cks-1 pulldown (Cks-1 PD) shown in panel A (15% of the total sample in each case), was immunoblotted for the indicated proteins. (C) Size-separated FPLC fractions from KB-3 cells treated with vinblastine (30 nM, 16 h) were immunoblotted for JNK1 and JNK2. A WCE from the same cells was also analyzed. The migration of a 45-kDa standard is shown. (D) FL62 was incubated with purified active JNK1 in a kinase reaction, subjected to peptide-PAGE, and analyzed by Coomassie blue staining and a phosphorimager. GST–c-Jun was used as a positive control, and the migration positions of GST–c-Jun and FL62 are indicated.

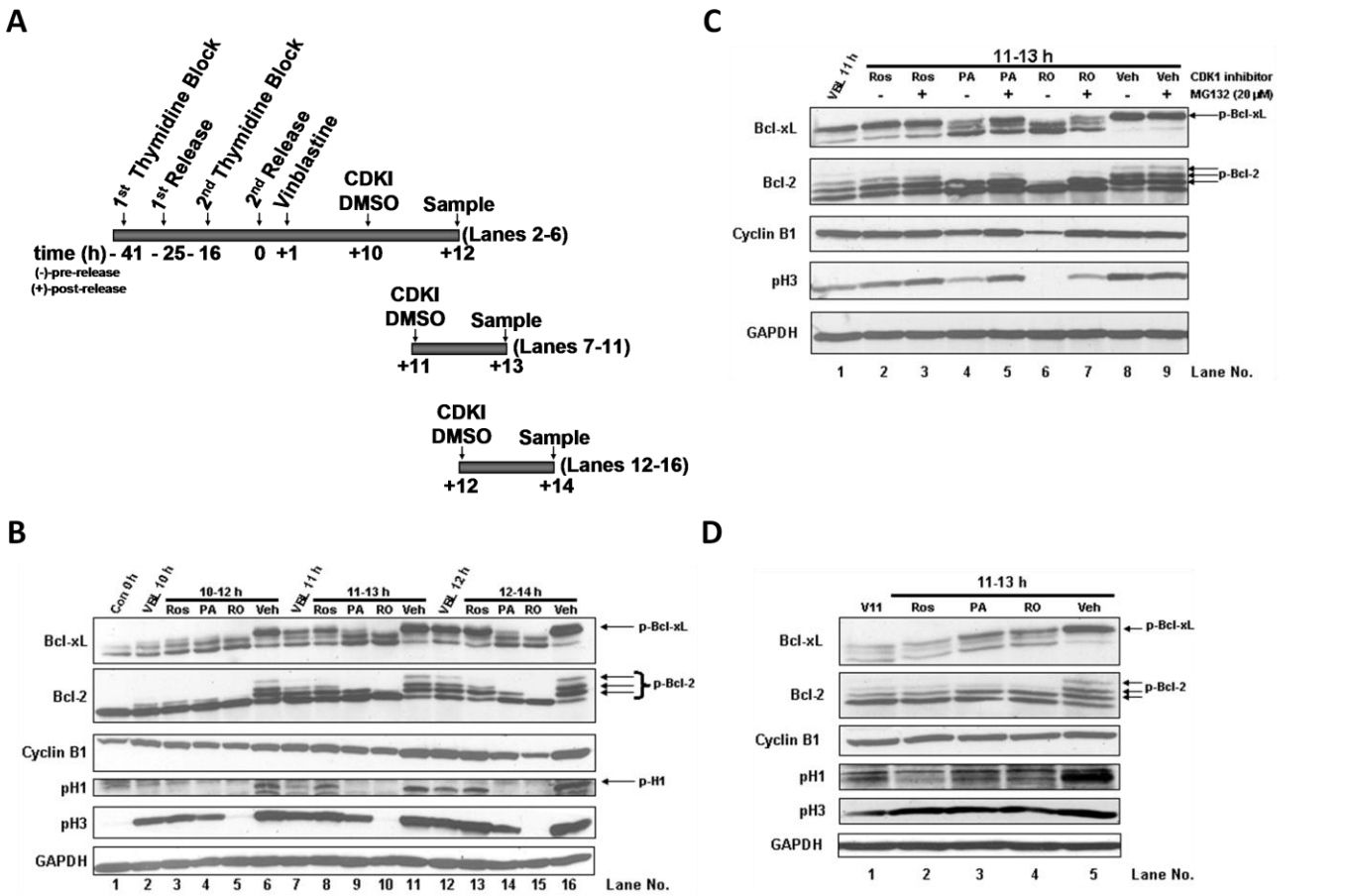

Fig. 2. Multiple CDK inhibitors inhibit vinblastine-induced Bcl-xL/Bcl-2 phosphorylation. (A) Experimental design. The timing of events for cell synchrony by a double thymidine block and cell cycle-specific timing of CDK1 inhibition following vinblastine treatment are shown. Lane numbers refer to panel B. (B) CDK inhibitors block Bcl-xL/Bcl-2 phosphorylation during mitotic arrest. KB-3 cells were synchronized at the G1/S boundary by a double thymidine block and were treated with 30 nM vinblastine (VBL) 1 h after release. Cells were harvested at 10 h, 11 h, 12 h, and 14 h after release or were treated with 25 μM Ros, 10 μMPA, 10 μMRO, or the DMSO vehicle (Veh) for 2 h during the periods from 10 to 12 h, 11 to 13 h, and 12 to 14 h after release. An untreated dish of cells harvested immediately after release from the double thymidine block (Con, 0 h) was included as a control. Arrows indicate phosphorylated forms of Bcl-xL, Bcl-2, or phospho-H1 histone. Whole-cell extracts were prepared and immunoblotted for the indicated proteins. GAPDH was used as a loading control. (C) CDK inhibitors maintain inhibition of Bcl-xL phosphorylation when the proteasome is inhibited. KB-3 cells were synchronized at the G1/S boundary by a double thymidine block and were treated with 30 nM VBL 1 h after release. Cells were harvested 11 h after release or were incubated for 2 h (i.e., from 11 to 13 h after release) with 25 μM Ros, 10 μM PA, 10 μM RO, or DMSO in the presence or absence of the proteasome inhibitor MG132 (20 μM). MG132 was added 20 min prior to the addition of the CDK inhibitors. Immunoblotting for the indicated proteins was performed. Arrows indicate phosphorylated (p) forms. (D) The CDKinhibitors PA and RO block Bcl-xL phosphorylation at concentrations that do not cause mitotic slippage. KB-3 cells were synchronized at theG1/S boundary by a double thymidine block and were treated with 30 nM VBL 1 h after release. Cells were harvested 11 h after release or were incubated for 2 h (i.e., from 11 to 13 h after release) with 25 μM Ros, 1 μM PA, 1 μM RO, or the DMSO vehicle. Immunoblotting for the indicated proteins was performed. Arrows indicate phosphorylated (p) forms.

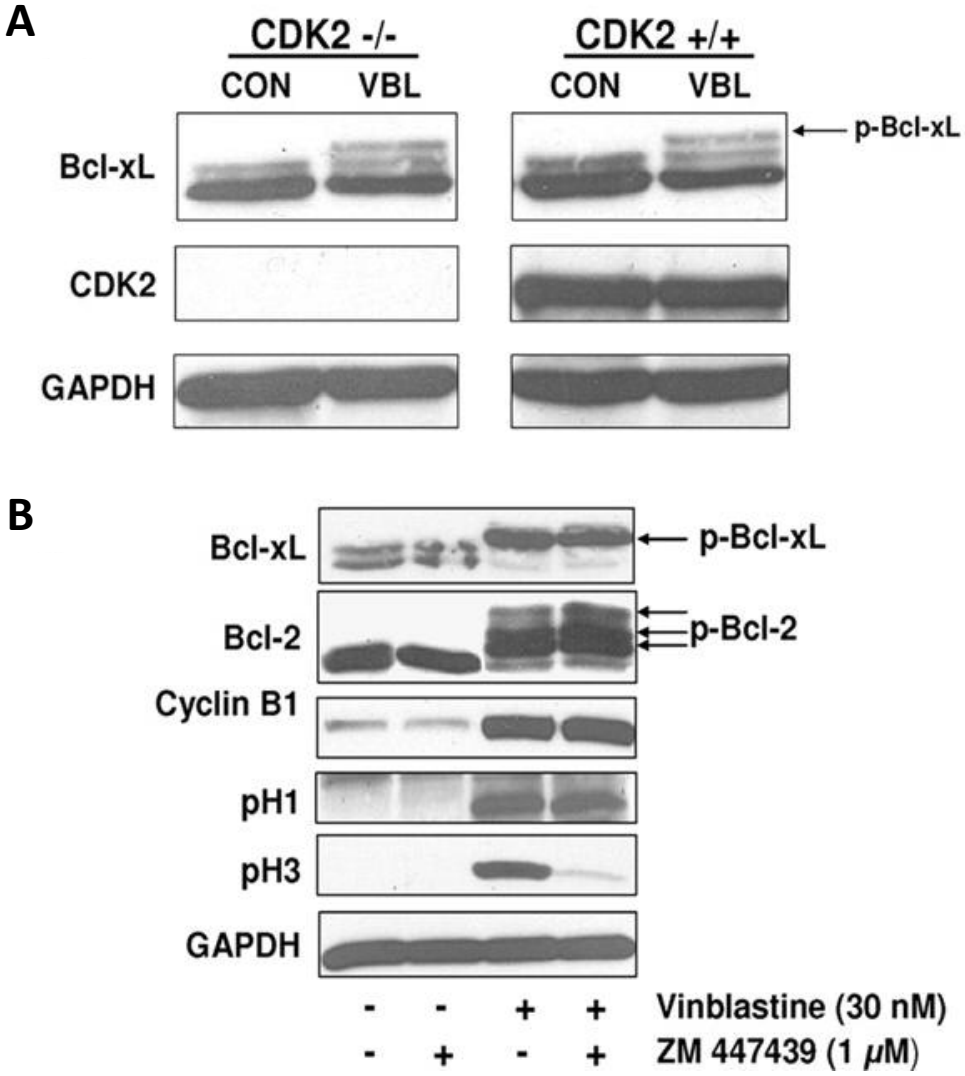

Fig. 3. Bcl-xL phosphorylation is independent of CDK2. (A) Wild-type (CDK2+/+) or CDK2-/- primary mouse embryonic fibroblasts were either left untreated (CON) or treated with 30 nM VBL for 8 h. Whole-cell extracts were prepared and immunoblotted for the indicated proteins. The molecular mass of CDK2 is 33 kDa. p-Bcl-xL, phosphorylated Bcl-xL. GAPDH was used as a loading control. (B) Inhibition of aurora kinase activity does not alter vinblastine-induced phosphorylation of Bcl-xL. KB-3 cells were synchronized at the G1/S boundary by a double thymidine block. Cells were either left untreated or were treated with 30 nM VBL 1 h after release. Nine hours after release, cells were either left untreated or treated with the aurora kinase inhibitor ZM44739 (1 μM). Cells subjected to all four conditions were harvested at 16 h postrelease, and whole-cell extracts were prepared and immunoblotted for the indicated proteins. pH1, phospho-H1 histone; pH3, phospho-H3 histone (Ser10). GAPDH served as a loading control.

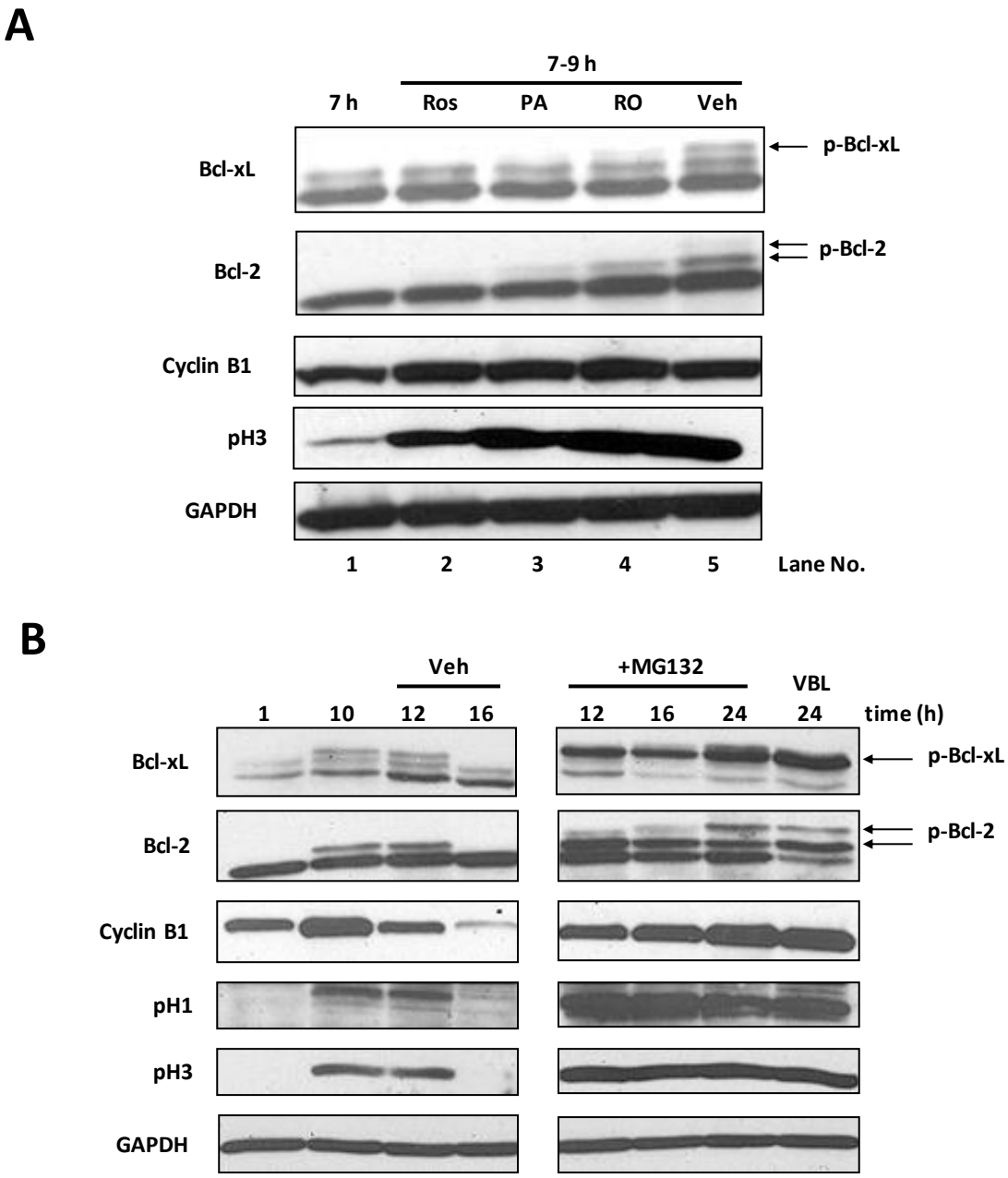

Fig. 4. CDK inhibitors inhibit mitotic Bcl-xL/Bcl-2 phosphorylation which is normally transient but sustained if mitosis is prolonged. (A)**.** Inhibition of CDK inhibits mitotic Bcl-xL/Bcl-2 phosphorylation. KB-3 cells were synchronized at the G1/S boundary by double thymidine block and at 7 h after release either harvested or treated for 2 h with 25 μM R-roscovitine (Ros), 1 μM purvalanol A (PA), 1 μM RO3306 (RO), or DMSO vehicle (Veh). Whole cell extracts were prepared and immunoblotted for the indicated proteins. Arrows indicate phosphorylated (p) forms of Bcl-xL or Bcl-2. GAPDH was used as a loading control. (B) Prolonging mitosis without microtubule inhibition leads to sustained Bcl-xL/Bcl-2 phosphorylation. KB-3 cells were synchronized at the G1/S boundary by double thymidine block and released into complete medium. Two flasks of cells were untreated and harvested at 1 h and 10 h post-release as controls. Other flasks of cells were treated with DMSO vehicle (Veh) or MG132 (20 μM) at 10 h post-release and harvested at the indicated time points following release. Whole cell extracts were prepared and immunoblotted for the indicated proteins. One flask of synchronized cells was treated with 30 nM vinblastine (VBL) for 24 h as a positive control for sustained mitotic arrest. Arrows indicate phosphorylated (p) forms of Bcl-xL or Bcl-2. GAPDH was used as a loading control

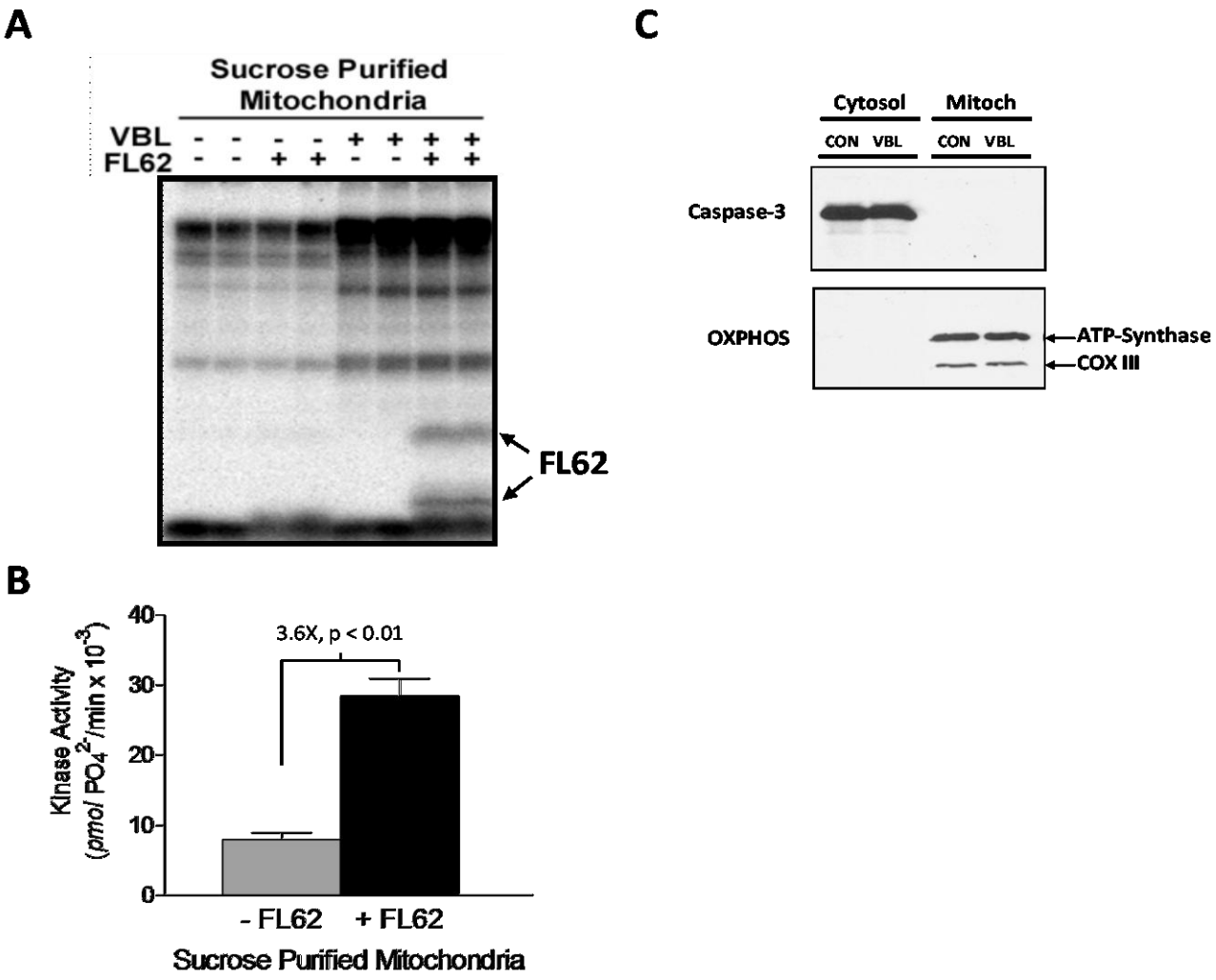

Fig. 5. FL62 kinase localizes to the mitochondria after vinblastine treatment. (A) KB-3 cells were untreated or treated with 30 nM vinblastine (VBL) for 16 h, mitochondrial fractions were prepared by sucrose density centrifugation, and incubated without or with FL62 in a radioactive kinase reaction in duplicate. Reactions were subjected to peptide-PAGE and phosphorimager analysis, with 24 h exposure. The higher and lower molecular weight forms of phosphorylated FL62 are indicated. (B) FL62 kinase activity in purified mitochondria from vinblastine treated cells. Assays were conducted in triplicate and ^{32}P incorporation determined by the P81 filter assay. Results are shown as mean ± S.D. with p-value. (C) Cytosolic and mitochondrial molecular markers. Cytosolic and mitochondrial fractions from control (CON) and vinblastine (VBL) samples in panel A were immunoblotted for cytosolic (Caspase-3) and the indicated mitochondrial markers from the oxidative phosphorylation complex (OXPHOS) of enzymes, including ATP Synthase (upper band) and Complex III (lower band).

APPENDIX 2: The following is the manuscript submitted to and accepted by the Molecular and Cellular Biology Journal in 2010. The text below is the final version and format in Microsoft Word that was used for print as a PDF and available on PubMed and the Molecular and Cellular Biology Journal website. Thus, the text is 11 point Times New Roman as requested by that journal. The formal reference available on PubMed is below.

- **Terrano, D.T**. and Chambers T.C. Cyclin-Dependent Kinase 1-Mediated Bcl-xL/Bcl-2 Phosphorylation Acts as a Functional Link Coupling Mitotic Arrest and Apoptosis. Mol. Cell. Biol., 2010, 30(3), 640-656. PMID 19917720.

Running title: CDK1-mediated Bcl-xL/Bcl-2 phosphorylation

David T. Terrano, Meenakshi Upreti, and Timothy C. Chambers*

From the

Department of Biochemistry and Molecular Biology

University of Arkansas for Medical Sciences

Little Rock, AR 72205

*Address correspondence to: Timothy Chambers, Department of Biochemistry and Molecular Biology, University of Arkansas for Medical Sciences, Mail Slot 516, and 4301 W. Markham St., Little Rock, AR 72205-7199. Tel: (501) 686-5755; Fax: (501) 686-8169.

E-mail: ChambersTimothyC@uams.edu

Materials and Methods (2,025 words); Introduction, Results, and Discussion (5,936 words)

Abbreviations: CDK, cyclin-dependent kinase; FPLC, fast-pressure liquid chromatography; IPTG, isopropyl-1-thio-β-D-galactopyranoside; MTI, microtubule inhibitor; PA, purvalanol A; Ros, roscovitine; RO, RO3306; GFP, green fluorescent protein; PARP, poly(ADP-ribose) polymerase.

ABSTRACT

Despite detailed knowledge of the components of the spindle-assembly checkpoint, a molecular explanation of how cells die after prolonged spindle checkpoint activation, and thus how microtubule inhibitors and other anti-mitotic drugs ultimately elicit their lethal effects, has yet to emerge. Mitotically arrested cells typically display extensive phosphorylation of two key anti-apoptotic proteins, Bcl-xL and Bcl-2, and evidence suggests that phosphorylation disables their anti-apoptotic activity. However, the responsible kinase has remained elusive. In this report evidence is presented that CDK1/cyclin B catalyzes mitotic arrest-induced Bcl-xL/Bcl-2 phosphorylation. Furthermore, we show that CDK1 transiently and incompletely phosphorylates these proteins during normal mitosis. When mitosis is prolonged in the absence of microtubule inhibition, Bcl-xL and Bcl-2 become highly phosphorylated. Transient overexpression of non-degradable cyclin B1 caused apoptotic death which was blocked by a phospho-defective Bcl-xL mutant but not by a phospho-mimic Bcl-xL mutant, confirming Bcl-xL as a key target of pro-apoptotic CDK1 signaling. These findings suggest a model whereby a switch in the duration of CDK1 activation, from transient during mitosis to sustained during mitotic arrest, dramatically increases the extent of Bcl-xL/Bcl-2 phosphorylation, resulting in inactivation of their anti-apoptotic function. Thus, phosphorylation of anti-apoptotic Bcl-2 proteins acts as a sensor for CDK1 signal duration and as a functional link coupling mitotic arrest to apoptosis.

INTRODUCTION

The cell division cycle is controlled by checkpoints, which ensure the fidelity of chromosome replication and segregation, and orderly progression through the cell cycle. If these critical events cannot be completed as scheduled, damaged cells, which might otherwise pose a threat to the organism as pre-cancerous cells, are eliminated (16). The mitotic checkpoint, for example, produces a "prevent anaphase" signal until all the chromosomes are properly attached to kinetochores (22). Microtubule inhibitors and other anti-mitotic agents prolong the activation of this checkpoint causing mitotic arrest, which culminates in cell death generally via intrinsic apoptosis, providing a rationale for their use as antitumor agents (20, 31). Intrinsic or mitochondrial apoptosis is regulated by the Bcl-2 family of proteins which exhibit either pro- or anti-apoptotic properties (17, 37). The BH3-only pro-apoptotic members act as essential initiators of intrinsic apoptosis, whereas the multidomain pro-apoptotic Bax and Bak act as essential mediators of mitochondrial membrane permeability. Anti-apoptotic Bcl-2 family members, including Bcl-xL, Bcl-2 and Mcl-1, oppose apoptosis by binding and neutralizing the activity of the pro-apoptotic members.

The molecular mechanisms leading to cell death in response to spindle checkpoint activation have yet to be established. Indeed, how the spindle checkpoint couples to pathways regulating cell survival and death still represents an unresolved issue in cell biology (26, 35). Nonetheless, it seems reasonable to hypothesize that signals generated in response to prolonged mitotic arrest are eventually transduced to the apoptotic machinery. In this regard, it is striking that microtubule inhibitors (MTIs) consistently induce the phosphorylation of two key anti-apoptotic proteins, Bcl-2 and Bcl-xL, whereas other apoptotic stimuli fail to do so (9, 13, 25). Results of studies with phospho-defective mutants of Bcl-2 and Bcl-xL indicate that phosphorylation antagonizes their anti-apoptotic function (2, 33, 36), but the precise mechanism(s) have yet to be fully clarified.

The identity of the kinase responsible for the extensive phosphorylation of Bcl-xL and Bcl-2 that occurs in response to sustained spindle checkpoint activation is unresolved. Identification of this kinase is considered to be of critical importance as it will provide insight into the molecular links between mitotic arrest and cell death as well as the molecular mechanism of action of anti-mitotic drugs. Several candidates have been proposed including Raf-1 (3), JNK (2, 11, 36), PKA (32), CDK1 (24), and mTOR (4). In general, however, conclusions have been correlative or based on the

use of kinase inhibitors tested under conditions which precluded mitotic arrest and which thus indirectly blocked the effects of MTIs, and strong experimental evidence supporting identification is lacking.

Here we present evidence that the CDK1/cyclin B kinase complex is responsible for mitotic arrest-induced Bcl-xL/Bcl-2 phosphorylation. Furthermore, we show that CDK1 transiently and incompletely phosphorylates these proteins during normal mitosis. The findings suggest a model whereby a switch in the duration of CDK1 activation, from transient during mitosis to sustained during mitotic arrest, dramatically increases the extent of Bcl-xL/Bcl-2 phosphorylation, resulting in inactivation of their anti-apoptotic function. Thus, CDK1-mediated phosphorylation of anti-apoptotic Bcl-2 proteins acts as a key link coupling mitotic arrest to apoptosis.

MATERIALS AND METHODS

Materials

Cyclin B1 (CAT# sc-245), CDK1 (CAT# sc-747), phospho-CDK1 (CAT# sc-12341), JNK1 (CAT# sc-474), JNK2 (CAT# sc-7345) and CDK2 (CAT# sc-163) antibodies were purchased from Santa Cruz; Bcl-xL (CAT# 2762), GAPDH (CAT# 2118) and phospho-H3 histone (Ser10) (CAT# 97015) antibodies were purchased from Cell Signaling; antibodies to cytochrome c (CAT# 55643), cyclin A (CAT# 14531A) and poly(ADP-ribose) polymerase (CAT# 556362) were purchased from Pharmingen; phospho-H1 histone antibody (CAT # 06-597) was from Upstate; and OXPHOS complex antibody (CAT# MS601) was from Molecular Probes. FITC-Donkey Anti Rabbit IgG (H+L) (CAT# 711-095-152) secondary antibody for immunofluorescence was purchased from Jackson ImmunoResearch. MitoTracker Red CMSRos (CAT# M7512) and DAPI (CAT# D-3571) stains were purchased from Molecular Probes. The Cdc kinase subunit (Cks-1) agarose conjugate (recombinant yeast $p13^{suc1}$ fused to GST and covalently linked to Sepharose^{TM} CL-4B) was purchased from Millipore. The peptide, FL62, with amino acid sequence HLADSPAVNRRR, was synthesized at 95% purity by Genscript. [γ^{32}P]ATP (250 μCi at 10 μCi/μl) was obtained from Perkin-Elmer. Calf thymus H1 histone was purchased from Calbiochem. Purified, activated JNK1 was obtained from Upstate Biotechnology and purified active CDK1/cyclin A2 was purchased from SignalChem. Pre-cast 16.5% acrylamide Tris/Tricine gels, in an 18-well format, were purchased from Bio-Rad. All drugs for treatment of cells, including vinblastine, Taxol, doxorubicin, vincristine, and colchicine, and the molecular weight standard kit (MW-GF-200) for size exclusion chromatography, were obtained from Sigma. Thymidine, MG132, isopropyl-1-thio-β-D-galactopyranoside (IPTG) and R-roscovitine were purchased from EMD Biosciences. Aminopurvalanol A and RO3306 were purchased from Axxora and ZM447439 was from Tocris Biosciences. *E. coli* strain BL21 (DE3) was purchased from Novagen.

Cell culture and synchronization

The KB-3 human carcinoma cell line and mouse embryonic fibroblasts (MEFs) were maintained in monolayer culture at 37 °C and 5% CO_2 in Dulbecco's modified Eagle's medium, supplemented with 10% fetal bovine serum, 2 mM L-glutamine, 50 units/ml penicillin, and 50 μg/ml streptomycin. KB-3 cells were synchronized by the double thymidine block method as described previously (10). Briefly, cells (10^6) were incubated in medium containing 2 mM thymidine for

16 h, released into normal medium for 9 h, and then incubated for 16 h in medium containing 2 mM thymidine. Release into fresh medium from this second block, with 98% of cells at the G_1/S boundary as determined by flow cytometry (10), was designated as time point 0 h.

Preparation of whole cell extracts and immunoblotting

To prepare whole cell extracts for kinase reactions or size exclusion chromatography, KB-3 cells were harvested, washed and pelleted twice with cold PBS (5 min at 500 x *g*), and resuspended in lysis buffer (25 mM HEPES, pH 7.5, 300 mM NaCl, 0.1% Triton X-100, 1.5 mM $MgCl_2$, 0.2 mM EDTA, 0.5 mM DTT, EDTA-free complete protease inhibitor tablets (Roche), 20 μg/ml aprotinin, 50 μg/ml leupeptin, 10 μM pepstatin, 1 mM phenylmethylsulfonyl fluoride, 20 mM β-glycerophosphate, 1 mM Na_3VO_4, and 1 μM okadaic acid). The suspension was incubated for 15 min on ice with occasional mixing, insoluble material was removed by centrifugation (20 min at 100,000 x *g*), and the supernatant was retained as the whole cell extract (WCE). Protein concentration was determined using the Bio-Rad protein assay. Immunoblotting was performed as described previously (11) with quantitation carried out using ImageJ software.

Size exclusion fast pressure liquid chromatography (FPLC)

Whole cell extracts were subjected to size exclusion chromatography on a Superdex 200 10/300 column by FPLC (Amersham) using a flow rate of 0.2 ml/min in 50 mM Tris-HCl, pH 7.5, 300 mM NaCl. UV absorbance at 280 nm was monitored during elution and fractions of 0.5 ml were collected in tubes containing Triton X-100 (0.1 % final concentration), glycerol (5% final), and protease and phosphatase inhibitors as above. Molecular weight standards were cytochrome c (12.4 kDa), carbonic anhydrase (29 kDa), albumin (66 kDa), alcohol dehydrogenase (150 kDa), β-amylase (200 kDa), and blue dextran (2000 kDa).

Kinase assays

For assessment of FL62 kinase activity in column fractions, aliquots of 22 µl were incubated without or with FL62 (50 µg) at 30˚C for 20 min in kinase reaction mix: 25 mM Tris-HCl, pH 7.5, 10 mM $MgCl_2$, 5 mM DTT, 1 µM ATP, and 1 µCi [γ^{32}P]ATP. Reactions were stopped by adding EDTA to 20 mM. For phosphorimage analysis, samples were boiled in SDS sample buffer and a maximum of 10 µl (a minimum of 10 µg of FL62 for Coomassie Blue visualization) was applied to 16.5% acrylamide Tris/Tricine high resolution gels (referred hereafter as peptide-PAGE). The gels were fixed in 5% glutaraldehyde overnight, washed extensively with dH_2O, and exposed to a phosphorimager screen. Control and samples from drug-treated cells were always analyzed side-by-side with the same reagents and exposures times. Fractions from the void volume served as negative controls. Whole cell extracts (5 µg protein) were assayed similarly with 10 µg FL62/reaction. For P81 phosphocellulose filter paper assays, the same incubation conditions were used except that reactions contained 10 µg FL62 and 0.1-1 µCi [γ^{32}P]ATP. After incubation, reactions were stopped by adding EDTA to 20 mM, acidified with 15% acetic acid, and spotted onto 2 cm P81 phosphocellulose filter discs (Fisher). Filters were washed with 75 mM H_3PO_4 (4 x 500 ml), air dried, and ^{32}P incorporation measured by scintillation counting. In vitro reactions with active JNK1 contained 1 unit of enzyme and either 15 µg FL62 or 1 µg GST-c-Jun in kinase reaction mix as above. After 20 min at 30°C, reactions were terminated by the addition of EDTA to 20 mM and subjected to peptide-PAGE and phosphorimage analysis. Immunocomplex assay of CDK1/cyclin B was conducted using whole cell extracts first pre-cleared with mouse IgG for 30 min at 4˚C, and then incubated with mouse anti-cyclin B1 antibody for 2 h at 4˚C, and then with mouse IgG agarose overnight at 4˚C. The pellets were washed twice with lysis buffer and subjected to kinase assays with FL62 (10 µg) or H1 histone (1 µg) as substrates as above. Separate immunoprecipitations were conducted for each reaction and blank values were obtained by excluding substrate.

Depletion of CDK with the Cdc kinase subunit-1 (Cks-1)

Whole cell extracts (400 µg) were incubated with Cks-1 agarose conjugate (20 µl) for 3 h at 4˚C, pelleted, and the supernatant was incubated again with Cks-1 agarose (20 µl) for 3 h at 4˚C. Extracts incubated for 6 h at 4˚C without Cks-1 agarose served as controls. CDK-depleted and control extracts were subjected to kinase assays with 1 µg H1 histone or

10 μg FL62 for 20 min at 30˚C in a kinase reaction mix with 10 μM ATP and 1 μCi [γ^{32}P]ATP. ^{32}P incorporation was determined by the phosphocellulose filter paper assay and scintillation counting as above.

Flow cytometry

To determine cell cycle distribution, cells were collected by trypsinization, fixed in 70% ethanol, washed in PBS, resuspended in 1 ml of PBS containing 1 mg/ml RNase and 50 μg/ml propidium iodide, incubated for 20 min in the dark at room temperature, and analyzed by flow cytometry using a FACSCalibur (Becton Dickinson, Mountain View, CA). The data were analyzed using the ModFit DNA analysis program (Verity Software House).

Preparation, phosphorylation and mass spectrometry of His-BclxL-ΔC

Recombinant His-BclxL-ΔC, which has an amino-terminal histidine tag and lacks the carboxy-terminal transmembrane domain to enhance solubility, was prepared using standard methodology. Briefly, E.coli strain BL21 (DE3) were transformed with pET29b-BclxL-ΔC plasmid and grown in 2×YT medium (50 ml) containing 10 μg/ml kanamycin and induced with 0.4 mM IPTG overnight at 30˚C. Bacterial pellets were lysed on ice for 30 min in 5 ml of 50 mM phosphate buffer containing 0.3 M NaCl, 10 mM imidazole, 1 mg/ml lysozyme, and protease inhibitors. The bacterial lysate was sonicated and cell debris was pelleted at 10,000 x *g* for 30 min. The cleared lysate was loaded onto a Qiagen NiNTA spin column and, after washing, the His-tagged protein was eluted with 250 mM imidazole. HisBclxL-ΔC containing fractions were pooled and dialyzed in Pierce Slide-A-Lyzer cassettes (Thermo Scientific) overnight at 4˚C against buffer containing 50 mM Tris-HCl, pH 7.5, 100 mM NaCl, 1 mM DTT, and 1 mM EDTA. Protein samples at a concentration of 1 mg/ml in 20% glycerol were stored at -70˚C.

HisBclxL-ΔC (5 μg) was tested as a CDK1 substrate by incubation in kinase reaction mix with [γ^{32}P]ATP and up to 320 ng purified CDK1/cyclin A2 at 30°C for 20 min. Reactions were subjected to SDS-PAGE, colloidal Coomassie staining, and phosphorimage analysis. To determine the site of phosphorylation, 5 μg HisBclxL-ΔC was incubated in kinase reaction mix containing 1 μM non-radioactive ATP with or without 320 ng purified CDK1/cyclin A2, resolved by SDS-PAGE, stained with colloidal Coomassie, and bands excised from the gel. Proteins in each SDS-PAGE gel slice were reduced in 10 mM Tris(2-Carboxyethyl) phosphine, alkylated in 50 mM iodoacetamide, and digested in-gel with AspN protease (Roche) for 4 h at 37^{o}C. Resulting peptide products were separated by reverse-phase liquid chromatography using a C18 column resin (Phenomenex) on a nanoLC-2D HPLC system (Eksigent Technologies) and

analyzed by MS/MS using an electrospray-interface LTQ XL-Orbitrap mass spectrometer (Thermo). Proteins identities were confirmed and phosphorylated amino acids identified by searching the IPI human database using the Mascot search engine (Matrix Sciences).

Subcellular fractionation and preparation of mitochondria

Cytosolic and mitochondrial fractions were prepared as described previously (8). Briefly, cells were harvested, washed in PBS, and resuspended in mitochondrial extraction buffer (MEB: 10 mM HEPES, pH 7.5, 210 mM mannitol, 70 mM sucrose, 1 mM EDTA supplemented with protease and phosphatase inhibitors). Cells were lysed in a nitrogen cavitation bomb at 400 psi for 5 min. This produced >95% lysis as determined by trypan blue staining. Cell debris and nuclei were removed by centrifugation (5 min at 2000 x *g*) to produce the post-nuclear supernatant. This was centrifuged at 13,000 x *g* for 15 min to pellet the total mitochondrial fraction, which was resuspended in 150-750 µl of MEB, depending on the amount of cells used. The supernatant was retained as the cytosol, which was further clarified at 100,000 x *g* for 1 h to remove insoluble material. To further purify mitochondria, the total mitochondrial fraction was layered over 1.2 M sucrose which was layered over 1.6 M sucrose. Both sucrose solutions were prepared in 10 mM Hepes, pH 7.5, 1 mM EDTA, and 0.1% BSA. The gradient was centrifuged at 27,000 rpm for 2 h in a Beckman SW28 rotor and mitochondria were recovered at the 1.2 M and 1.6 M sucrose interface and washed twice in MEB.

Immunofluorescence

Cells plated on glass coverslips were incubated with 30 nM MitoTracker Red for 20 min, which was replaced with fresh media for 1.5 h and then changed again for 10 min. For vinblastine treated samples, MitoTracker Red was added 2 h prior to harvest at 16 h of treatment. The remaining staining procedure was conducted at room temperature. The plates were washed twice with PBS and cells were fixed and permeabilized with a 4% paraformaldyde/0.18% Triton-X100 solution for 30 min. The cells were washed three times with PBS and blocked with a solution of 1% BSA in PBS for 30 min, washed three times with PBS, and then incubated with polyclonal CDK1 primary antibody (1:50 dilution) or monoclonal cyclin B primary antibody (1:100 dilution) for 1 h. The cells were washed three times with PBS and incubated with FITC goat anti-rabbit secondary antibody (1:100) for 1 h. The cells were washed three times with PBS and nuclei were stained

with DAPI for 5 min, followed by three washes with PBS. Immunofluorescent protein (green), mitochondria (red), and nuclei (blue) were visualized using 488, 561, and 405 nm laser lines, respectively, of a Zeiss LSM410 confocal microscope, and images processed using Adobe Photoshop.

Transient transfections and apoptosis assays

KB-3 cells were transiently transfected with plasmid DNA using a combination of Lipofectamine and Lipofectamine Plus reagents (Invitrogen) according to manufacturers' instructions. Cells were harvested 48 h after transfection for apoptotic cell death assay and after 24 or 48 h for detection of expressed proteins by immunoblotting. Apoptosis was determined using a cell death detection enzyme-linked immunosorbent assay kit (Roche Applied Science) as previously described (33). This is a quantitative photometric immunoassay for the determination of cytoplasmic histone-associated oligonucleosomes generated during apoptosis.

RESULTS

Validation of FL62 as a peptide substrate of the Bcl-xL kinase

Recently, we identified by protein purification and mass spectrometry the major vinblastine-induced phosphorylation site in Bcl-xL to be Ser62 (33), in the flexible loop (FL) region between the BH3 and BH4 domains (37). We reasoned that a small peptide encompassing this site might act as a useful and specific substrate to facilitate identification of the vinblastine-activated Bcl-xL kinase. A peptide, denoted FL62, was synthesized that encompasses residues 58-66 of human Bcl-xL, with three arginines added to the carboxy-terminus to facilitate binding to phosphocellulose filters (Fig. 1A). The 1.4 kDa peptide (molecular weight confirmed by mass spectrometry) could be visualized by Coomassie staining after electrophoresis using peptide-PAGE, as described in Materials and Methods, where it migrated with an apparent molecular weight of about 2.5 kDa (Fig. 1B). In order to test the peptide as a substrate, protein extracts from untreated and vinblastine-treated KB-3 cells were size-fractionated by FPLC using a Superdex-200 column, and fractions were incubated under phosphorylation conditions with or without FL62. Samples were subjected to peptide-PAGE and phosphorimage analysis. Significant phosphorylation of FL62 was observed in extracts from vinblastine treated cells and not from control cells, with peak activity at fraction 24 (Fig. 1C). Interestingly, the phosphorylated peptide migrated as two distinct bands on these gels (approximately 2.5 kDa and 7.5 kDa), with the slower migrating band containing most of the ^{32}P radioactivity (Fig. 1C), and the faster migrating band corresponding to the bulk of the peptide as judged by Coomassie staining (data not shown). While the basis for this observation is unclear, it appears that phosphorylation may alter the conformation and/or SDS binding properties of the peptide, or may promote the formation of FL62 oligomers.

Initial characterization of FL62 kinase and relationship to Bcl-xL phosphorylation

In order to further characterize the FL62 kinase, and to avoid time-consuming assays involving gel electrophoresis that required prolonged fixation and extensive washing steps, a rapid P81 phosphocellulose filter disc method was tested. Re-assay of the FPLC fractions confirmed that this method provided a robust and specific signal that precisely paralleled the peak of kinase activity observed in the peptide gels (Fig. 2A). Since Bcl-xL phosphorylation is widely induced by MTIs (25), extracts from Taxol-treated cells were subjected to the same analysis. The same profile of FL62 kinase activity, again peaking at fraction 24, was observed (Fig. 2B). The absence of FL62 kinase activity in samples from cells treated

with vinblastine for 48 h, a time-point where cellular Bcl-xL has become dephosphorylated (9), also supported a correlation between FL62 kinase activity and the phosphorylation status of cellular Bcl-xL (Fig. 2B). The profile of FL62 kinase activity from the Superdex column in relation to the protein absorbance profile and the elution of molecular mass standards provided an estimate of native molecular weight in the range 150-190 kDa (Fig. 2C).

To further document the drug specificity of FL62 kinase activation, cells were treated with doxorubicin, a DNA interchelator and topoisomerase inhibitor that does not induce mitotic arrest in KB-3 cells (9). Cell extracts were subjected to size exclusion FPLC and FL62 kinase assay. FL62 phosphorylation was essentially undetectable in the extract from doxorubicin-treated cells (Fig. S1A), similar to that found for untreated cells (Fig. 1C). As previously reported (9), doxorubicin failed to induce Bcl-xL phosphorylation, despite an ability to induce apoptosis, as judged by PARP cleavage (Fig. S1B). Taken together, these results indicate that the FL62 kinase assay specifically detects the MTI-activated kinase responsible for Bcl-xL phosphorylation in vivo.

Relationship to mitotic arrest

In order to facilitate analysis of multiple samples, we tested whether FL62 kinase activity could be detected in whole cell extracts. FL62 phosphorylation was readily observed when extracts derived from vinblastine treated cells, but not untreated cells, were used as a source of kinase activity (Fig. 3A). Treatment of KB-3 cells with increasing concentrations of vinblastine indicated a dose-dependent response up to a maximum at 10 nM vinblastine with no further increase in kinase activity at higher drug concentrations (Fig. 3B; black bars). The expression of cyclin B (dotted line in upper panel, blot in lower panel, Fig. 3B) and the percentage of cells with 4N DNA content (Fig. 3B) showed a dose-dependency strikingly similar to that of the kinase activity which also closely paralleled the level of Bcl-xL phosphorylation (Fig. 3B). These results suggest that the degree of activation of FL62 kinase is directly related to the extent of mitotic arrest and not to the vinblastine concentration *per se*, and that kinase activity is also closely correlated with phosphorylation of cellular Bcl-xL.

FL62 kinase activation and Bcl-xL phosphorylation during normal mitosis

As FL62 kinase activity correlated with the degree of mitotic arrest, we explored whether the enzyme was also active during normal mitosis. Mitotic KB-3 cells were prepared by synchronizing them with the double thymidine block method and releasing them into medium and harvesting 10 h later, which corresponds to M phase (9). Extracts were prepared and assayed for FL62 kinase activity. Mitotic cells showed a significant 4-fold increase in FL62 kinase activity compared to asynchronous cells, while extracts from vinblastine treated cells showed a 13-fold increase (Fig. 4A). Analysis of Bcl-xL from these same samples showed that, while control cells and vinblastine treated cells had unphosphorylated and fully phosphorylated Bcl-xL, respectively, Bcl-xL from mitotic cells was intermediate, with a roughly equal proportion of both unphosphorylated (lowest band) and phosphorylated (uppermost band) Bcl-xL (Fig. 4B). Thus, in mitotic cells, an incomplete level of Bcl-xL phosphorylation was observed in parallel with a relatively modest activation of FL62 kinase.

Next a more comprehensive experiment was conducted where several flasks of cells were synchronized at the G1/S boundary, with different sets released into medium containing either vehicle or vinblastine, and harvested at defined time points thereafter. During the 9-12 h period post-release, which comprised late G2 phase into mitosis and the beginning of the next G1 phase (10), in the control set, Bcl-xL underwent partial and transient phosphorylation (Fig. 4C, see arrowhead). This occurred in close concert with cyclin B expression levels, and did not correlate with cyclin A expression, which peaked earlier at 7-8 h post-release (Fig. 4C). When released in the presence of vinblastine, Bcl-xL underwent complete and sustained phosphorylation, and this again occurred in concert with sustained cyclin B expression, and was unrelated to cyclin A expression, which diminished to near undetectable levels by 16 h (Fig. 4C). Bcl-2 showed an essentially identical profile of phosphorylation, with partial and transient phosphorylation during normal mitosis versus sustained (and in this case, multi-site) phosphorylation following vinblastine treatment (Fig. 4C). Thus, vinblastine-induced mitotic block alters the temporal kinetics and extent of Bcl-xL/Bcl-2 phosphorylation, from transient and incomplete during normal mitosis, to sustained and complete, and this closely parallels cyclin B but not cyclin A expression.

FL62 kinase corresponds to CDK1/cyclin B

The temporal and quantitative relationship between FL62 kinase activity and Bcl-xL/Bcl-2 phosphorylation during mitosis and mitotic arrest suggested that CDK1, and more specifically CDK1/cyclin B, may be the FL62 kinase. Several experiments were conducted to explore this relationship further. First, FL62 kinase activity was found to co-elute from the Superdex 200 column with active CDK1/cyclin B complexes (Fig. S2). In addition, FL62 was an excellent *in vitro* CDK1 substrate, comparable to histone H1 (Table 1). To demonstrate more conclusively that FL62 kinase was a CDK, the Cdc kinase subunit (Cks-1) protein $p13^{suc1}$ from yeast conjugated to agarose, which directly binds CDKs (14), was used to deplete CDKs from whole cell extracts of vinblastine treated KB-3 cells. Kinase activities using both FL62 and H1 histone as substrates were measured in the original extract and following depletion. FL62 and H1 kinase activities decreased similarly, by over 50%, following CDK depletion (Fig. 5A). Immunoblotting showed that CDK1 and cyclin B were present in the Cks-1 pellet, and furthermore, these proteins were roughly equally distributed between the pellet and the supernatant following depletion (Fig. 5B), quantitatively consistent with the depletion of kinase activity. JNK1, on the other hand, was retained in the supernatant and was undetectable in the Cks-1 pellet (Fig. 5B), demonstrating the specificity of Cks-1, and excluding JNK as the FL62 kinase. To further confirm that the FL62 kinase corresponded to CDK1/cyclin B, cyclin B was immunoprecipitated and H1 histone and FL62 kinase activities measured in the immunoprecipitated material. As shown in Fig. 6A, mitotic extracts demonstrated significantly elevated CDK1/cyclin B kinase activity toward both substrates as compared to control extracts, and CDK1/cyclin B kinase activity was increased further in extracts from vinblastine-treated cells. While maximum CDK1 activity may be expected in both mitotic extracts and in extracts from mitotically arrested cells, this was not observed, and we consistently found greater CDK1 activity with either substrate in mitotically arrested cells (Fig. 4A, Fig. 6A, and data not shown). This observation may reflect the fact that untreated cells harvested at 10 h post-release may differ from one another, to some degree, with respect to proximity to M phase. In support of this possibility, CDK1 activation appeared more complete in extracts from vinblastine treated cells versus mitotic extracts, as judged by CDK1 gel mobility, where the faster migrating species represents the dephosphorylated, catalytically active form of the kinase (Fig. 6B).

FL62 kinase is distinct from JNK

Evidence both for and against the stress activated and proline directed kinase, c-Jun NH_2-terminal kinase (JNK), as the kinase responsible for MTI-induced Bcl-2/Bcl-xL phosphorylation has been reported (2, 9, 11, 36). The data of Fig. 5 indicated that FL62 kinase activity was not due to JNK activity. This conclusion was supported by probing Superdex-200 FPLC fractions for JNK1 and JNK2 immunoreactivity. JNK1 was mostly present in fractions 30-32 with a peak at fraction 31, while JNK2 eluted earlier in fractions 28-30, with a peak at fraction 29 (Fig. S3A), in contrast to FL62 kinase activity which was mainly detectable in fractions 23-25 (Fig. 1C). FL62 was also tested as a substrate for activate recombinant JNK1 and no detectable phosphorylation was observed, whereas an authentic substrate, GST-c-Jun, was readily phosphorylated (Fig. S3B). Thus FL62 kinase is distinct from JNK isozymes and FL62 is an ineffective substrate for JNK.

CDK inhibitors inhibit vinblastine-induced Bcl-xL/Bcl-2 phosphorylation

Next, we tested whether vinblastine-induced phosphorylation of cellular Bcl-xL and Bcl-2 occurred in a CDK1-dependent manner. For this purpose, several validated CDK inhibitors were selected, including roscovitine (Ros) (19), purvalanol A (PA) (27), and RO-3306 (RO) (34). Because these compounds inhibit CDKs in general, it was reasoned that they may delay or block cell cycle progression to M phase, and thus prevent Bcl-xL/Bcl-2 phosphorylation indirectly. To avoid this potential problem, cells were synchronized by double thymidine block, treated with vinblastine 1 h after release from G1/S phase, and then the CDK inhibitors were added later, for a short duration at several time points corresponding to late G2 and M phase. Specifically, the CDK inhibitors, or DMSO vehicle, were added for 2 h at 10, 11, or 12 h following G1/S release in the presence of vinblastine. This experimental strategy is depicted in Fig. 7A. Extracts were made and subjected to immunoblotting for Bcl-xL, Bcl-2, cyclin B1, phospho-H1 histone (a marker of CDK1 activity), and phospho-H3 histone (a marker of mitosis). These data are shown in Fig. 7B. Lane 1 shows the baseline, that is, blots performed from cell extracts at the time of second release (zero hour). Comparison of lane 2 and lane 6 shows that vinblastine induced a marked increase in Bcl-xL and Bcl-2 phosphorylation during the interval 10 h to 12 h post-release, as expected. In the presence of CDK inhibitors during this interval, Bcl-xL/Bcl-2 phosphorylation was strongly inhibited (compare lanes 3, 4 and 5 with lane 6). H1 histone phosphorylation showed a similar inhibitory profile. Blotting for

phospho-H3 histone showed that levels increased from 10 to 12 h (compare lane 2 and lane 6), and that Ros or PA treatment during this interval maintained phospho-H3 histone at initial (10 h) levels. However, after RO treatment, phospho-H3 histone levels were markedly diminished (compare lane 2 and lane 5), suggesting that RO may be causing mitotic slippage. Examination of the data obtained at 11 to 13 h after G1/S release in the presence of vinblastine (lanes 7-11 in Fig. 7B) was additionally revealing. During this interval, Bcl-xL/Bcl-2 phosphorylation increased markedly (compare lanes 7 and 11) and Ros blocked this increase without affecting phospho-H3 histone level and hence without causing mitotic exit. In contrast, PA and RO caused a reversal of Bcl-xL/Bcl-2 phosphorylation, and in concert, appeared to promote mitotic exit as judged by a reduction in phospho-H3 histone and cyclin B levels (compare lanes 8, 9 and 10 with lane 11). Examination of the data obtained during the interval 12-14 h showed that Bcl-xL/Bcl-2 phosphorylation was close to maximum at 12 h, and Ros blocked the modest increase occurring over the next 2 hours, while PA and RO again caused a reversal of Bcl-xL/Bcl-2 phosphorylation by inducing exit (Fig. 7B, lanes 12-16).

Inhibition of Bcl-xL/Bcl-2 phosphorylation is not a consequence of mitotic slippage

Results with the CDK1 inhibitors shown in Fig. 7B strongly suggested that the reversal of Bcl-xL/Bcl-2 phosphorylation caused by RO and PA, coinciding with a loss of H3 histone phosphorylation and a decrease in cyclin B1 expression, was a consequence of mitotic slippage. Furthermore, previous work has indicated that RO, the most potent of the three CDK1 inhibitors *in vitro* (RO, IC_{50} = 20 nM; PA, IC_{50} = 33 nM; Ros, IC_{50} = 650 nM), can potently cause mitotic slippage (34). Dephosphorylation of Bcl-xL and Bcl-2 as a result of mitotic slippage complicates interpretation of the effect of the CDK inhibitors on phosphorylation of these proteins. To clarify this issue, the proteasome inhibitor MG132 was used to prevent cyclin B degradation and subsequent mitotic slippage. KB-3 cells were synchronized, treated with vinblastine, and treated with the CDK1 inhibitors in the presence or absence of MG132 pretreatment (Fig. 7C). The increase in Bcl-xL/Bcl-2 phosphorylation occurring during the interval 11-13 h post-release (compare lanes 1 and 8 in Fig. 7C) was blocked in the presence of Ros (lane 2), and this was unaffected by the proteasome inhibitor (lane 3). Also consistent with the earlier results of Fig. 7B, PA and RO reversed to some degree vinblastine-induced Bcl-xL/Bcl-2 phosphorylation (Fig. 7C, lanes 4 and 6). However, in the presence of MG132, dephosphorylation was rescued (lanes 5 and 7), and the phosphorylation level of Bcl-xL/Bcl-2 was maintained at approximately the original control level (lane 1, Fig. 7C) and similar to the level of inhibition by Ros alone (lane 2). In addition, MG132 rescued PA- and RO-induced loss of cyclin B

and phospho-H3 histone, confirming that the proteasome inhibitor prevented mitotic slippage induced by these CDK inhibitors. Further, H1 histone phosphorylation was still susceptible to inhibition by the CDK inhibitors in the presence of MG132. Overall, these results show that inhibiting CDK1 activity while the cells are still mitotically arrested inhibits Bcl-xL/Bcl-2 phosphorylation.

The concentrations of PA and RO (10 μM) used in cell culture experiments described above are 300- and 500-fold greater than their *in vitro* IC_{50} values for CDK1, respectively (PA = 33 nM, RO = 20 nM). Because Ros, when used at ~30-fold greater than its IC_{50} for CDK1 (650 nM), effectively inhibited CDK1 without causing mitotic slippage, we tested whether lower concentrations of PA and RO would achieve a similar outcome. As shown in Fig. 7D, this was indeed the case. PA and RO used at 1 μM strongly inhibited vinblastine-induced Bcl-xL/Bcl-2 phosphorylation as well as H1 histone phosphorylation occurring at 11-13 h post-release, under conditions where mitotic slippage was prevented, as shown by maintenance of cyclin B and phospho-H3 histone levels. Collectively, the results of Fig. 7 provide compelling evidence that vinblastine-induced Bcl-xL/Bcl-2 phosphorylation is mediated via a CDK1-dependent pathway.

CDK-dependent mitotic Bcl-xL/Bcl-2 phosphorylation

To determine if mitotic Bcl-xl/Bcl-2 phosphorylation was similarly CDK-dependent, KB-3 cells were synchronized by double thymidine block, and at 7 h post-release, treated for 2 h with DMSO vehicle, 25 μM Ros, 1 μM PA or 1 μM RO. As shown in Fig. 8A, each of the CDK inhibitors blocked the increase in Bcl-xL/Bcl-2 phosphorylation occurring during this interval while maintaining phospho-H3 histone levels. These results suggest that mitotic Bcl-xL/Bcl-2 phosphorylation is also mediated by a CDK-dependent pathway.

Prolonging mitosis in the absence of microtubule inhibition is sufficient to induce extensive Bcl-xL/Bcl-2 phosphorylation

The finding that Bcl-xL and Bcl-2 are both partially and transiently phosphorylated during mitosis suggests the intriguing possibility that the extensive phosphorylation observed in response to MTIs is due to the prolonging of a CDK-mediated signal initiated in mitosis. To test this hypothesis, we used the proteosome inhibitor MG132 to block cyclin B

degradation. Specifically, KB-3 cells were synchronized by the double thymidine block method, and at 10 h post-release, after mitotic phosphorylation was initiated but before dephosphorylation had occurred (Fig. 4C), cells were treated with either vehicle or MG132 (Fig. 8B). In vehicle treated cells, partial and transient phosphorylation of Bcl-xL and Bcl-2 was observed, in concert with transient increases in cyclin B1, phospho-H1, and phospho-H3 levels. In MG132 treated cells, in contrast, much more extensive phosphorylation of Bcl-xL and Bcl-2 was observed, in parallel with sustained accumulation of cyclin B and sustained phosphorylation of H1 and H3 histones. Indeed, the levels of phosphorylation of Bcl-xL and Bcl-2 observed when mitosis was prolonged by MG132 in this manner approached those observed after treatment with vinblastine (Fig. 8B, far right lane). Thus, in the absence of microtubule inhibition, prolonging mitosis is sufficient to drive phosphorylation of Bcl-xL/Bcl-2 to high levels.

Vinblastine induces Bcl-xL phosphorylation in CDK2 null cells

The temporal kinetics of vinblastine-induced Bcl-xL phosphorylation coincided with CDK1/cyclin B activation. As further support for this identification, and to exclude other CDKs, wild-type ($CDK^{+/+}$) and CDK2 null ($CDK2^{-/-}$) primary MEFs were treated with vinblastine and Bcl-xL phosphorylation was analyzed. After 8 h of vinblastine treatment, a time-point found to be optimal, both $CDK2^{+/+}$ and $CDK2^{-/-}$ MEFs displayed comparable levels of Bcl-xL phosphorylation (Fig. S4). In contrast to KB-3 cells, however, phosphorylation was incomplete, with only a partial shift of the fastest migrating band (unphosphorylated Bcl-xL) to the slowest moving band (phosphorylated Bcl-xL), estimated to be 15% after quantitation. This partial response closely reflected the cellular response, in that only 10-15% of MEFs in the population appeared affected by the drug, showing rounding and loss of adherence, whereas the majority were morphologically normal. Such non-responsiveness may be because primary fibroblasts have a tendency to become quiescent in culture and thus refractory to cell cycle inhibitors. Thus, while the extent of Bcl-xL phosphorylation appeared to be cell-type specific, the highly similar response of both $CDK2^{+/+}$ and $CDK2^{-/-}$ MEFs indicates that CDK2 is not required for vinblastine-induced Bcl-xL phosphorylation.

Inhibition of aurora B does not affect vinblastine-induced Bcl-xL/Bcl-2 phosphorylation The data presented above show that Bcl-xL/Bcl-2 phosphorylation can be inhibited by CDK inhibitors in mitotically arrested cells where H3 histone phosphorylation is maintained. Mitotic H3 histone phosphorylation at Ser10 is catalyzed by the Ser/Thr spindle

checkpoint aurora B kinase (15). To further determine whether Bcl-xL/Bcl-2 phosphorylation and H3 histone phosphorylation were independent aspects of mitotic checkpoint signaling, and to test aurora B as a candidate Bcl-xL kinase, a small molecular inhibitor of aurora B, ZM447439, was utilized. Cells were synchronized by double thymidine block, treated with vehicle or vinblastine at 1 h post-release, then vehicle or ZM447439 was added 9 h post-release, and cells harvested 16 h post-release. As shown in Fig. S5, ZM447439 inhibited H3 histone phosphorylation without affecting Bcl-xL, Bcl-2 or H1 histone phosphorylation, or cyclin B expression. This experiment argues against aurora B as a candidate Bcl-xL kinase, and shows that under conditions where H3 histone phosphorylation is inhibited but mitotic slippage prevented, Bcl-xL/Bcl-2 phosphorylation levels are also maintained.

In vitro phosphorylation of full length Bcl-xL by CDK1

The results presented above show that CDK1 can directly phosphorylate Ser62 in the context of the peptide substrate FL62 in vitro and that mitotic and vinblastine-induced Bcl-xL/Bcl-2 phosphorylation in vivo occur in a CDK1-dependent manner. However, it remains possible that CDK1 fortuitously phosphorylates FL62 and that a CDK-activated kinase acts as an intermediate to phosphorylate Bcl-xL/Bcl-2 in vivo. To distinguish these possibilities, we tested whether full length Bcl-xL acted as a direct CDK substrate. Recombinant His-BclxL-ΔC, which has an N-terminal histidine tag and lacks the C-terminal transmembrane domain to enhance solubility, was incubated with increasing amounts of CDK1 in the presence of [γ^{32}P]ATP. Analysis of ^{32}P incorporation showed that His-BclxL-ΔC was phosphorylated by CDK1 in a dose-dependent manner (Fig. 9A). The reaction was replicated with non-radioactive ATP in the presence or absence of CDK1 for an extended incubation time of 5 h, the protein was excised from SDS gels (Fig. 9B), and analyzed by mass spectrometry after AspN digestion. In the covered sequence (51%), phosphorylation was detected only on Ser62 (Fig. 9C), and was undetectable in control reactions without CDK1 (data not shown). No phosphorylation of Thr47, another potential CDK site within the covered sequence, was observed. Thus CDK1 directly phosphorylates full-length Bcl-xL on the physiologically relevant site, Ser62.

Mitochondrial localization of CDK1/cyclin B

In order to extensively phosphorylate Bcl-xL and Bcl-2 during mitotic arrest, CDK1 would be predicted to localize or translocate to the mitochondria, where these proteins are predominately located (9), after vinblastine treatment.

Subcellular fractionation and immunofluorescent microscopy were used to test this prediction. Mitochondria were prepared and purified by sucrose density sedimentation and subject to in vitro phosphorylation in the absence or presence of FL62. Analysis of the samples by peptide-PAGE showed FL62 kinase activity in mitochondria from vinblastine-treated but not control cells (Fig. 10A). Quantitation of phosphate incorporation into FL62 by the phosphocellulose paper binding method was also performed. The results demonstrated an increase of 3.6-fold in phosphate incorporation in the presence versus absence of FL62 in the reaction mixtures (Fig. 10B). Caspase-3 and enzymes from the oxidative phosphorylation complex (OX-PHOS) were used as cytosolic and mitochondrial markers, respectively, to show lack of cross-contamination in the subcellular fractions (Fig. 10C).

Immunofluorescence microscopy (Fig. 10D) revealed that in control cells, CDK1 (green signal) was mainly coincident with nuclei (blue signal, DAPI) and distinct in location from mitochondria (red signal). In vinblastine treated cells, in contrast, a more diffuse pattern of CDK1 localization was observed, with extranuclear staining evident some of which coincided with the red mitochondrial signal. Localization of CDK1 to mitochondria was particularly evident in vinblastine-treated cells displaying condensed chromatin, i.e. mitotically arrested cells, as observed by DAPI staining (arrows in Fig. 10D, lower right panels). Examination of cyclin B by immunofluorescence microscopy revealed elevated levels after vinblastine treatment, which in part colocalized with mitochondria, particularly in cells with condensed nuclei (Fig. 10E). Thus CDK1/cyclin B complexes localize to the mitochondria in cells undergoing mitotic arrest.

Phospho-defective Bcl-xL blocks cell death induced by non-degradable cyclin B1

To directly test the hypothesis that Bcl-xL is a key target of pro-apoptotic CDK1 signaling, KB-3 cells were transiently transfected with a plasmid encoding non-degradable cyclin B1 (cyclin B1(R42A)-GFP). Plasmids encoding GFP or wild-type cyclin B1-GFP were used as controls. Fluorescent microscopy 24 h post-transfection demonstrated 50-60% transfection efficiency (data not shown) and immunoblotting showed elevated cyclin B1 expression after 24 h (Fig. 11A) which was maintained up to 48 h (data not shown). Apoptotic assays conducted 48 h post-transfection showed that cyclin B1(R42A)-GFP strongly induced cell death, as did wild-type cyclin B1 to a lesser extent, and this was independently confirmed by analysis of PARP cleavage (Fig. 11A). Next, cells were co-transfected with cyclin B1(R42A)-GFP together with wild-type, phospho-defective (S62A), or phospho-mimic (S62D) HA-Bcl-xL. Comparable expression of the Bcl-xL

constructs was demonstrated by immunoblotting for HA tag (Fig. 11B). Cyclin B1(R42A)-GFP-induced apoptotic cell death was strongly inhibited by S62A-Bcl-xL expression ($p \leq 0.001$ relative to wild-type Bcl-xL), whereas expression of S62D-Bcl-xL failed to protect cells ($p \leq 0.422$, not significantly different from wild-type Bcl-xL) (Fig. 11B). These results were independently confirmed by analysis of PARP cleavage (Fig. 11B). The data of Fig. 11 provide strong evidence that Bcl-xL acts as a key substrate for CDK1 pro-apoptotic signaling.

DISCUSSION

Extensive phosphorylation of Bcl-xL and Bcl-2 occurs in association with mitotic arrest across a broad spectrum of cell types, and evidence suggests that phosphorylation disables their anti-apoptotic function (2, 33, 36). Given the key role of these modifications in regulating apoptotic death of mitotically arrested cells, and given the need for illumination of the molecular and functional connections between mitotic arrest and apoptosis, identification of the responsible kinase is of obvious significance. However, while several candidates have been proposed (see Introduction), much of the evidence has been indirect and correlative, and no studies on isolation or characterization of the kinase have been reported. By developing and validating a specific assay to enable enzyme characterization, we present evidence here that CDK1/cyclin B is the kinase responsible for the extensive phosphorylation of Bcl-xL and Bcl-2 that occurs in mitotically arrested cells.

Data in support of this conclusion were derived from several experimental approaches. First, as demonstrated by Cks-1 depletion, FL62 kinase activity was clearly due to CDK activity. Evidence that FL62 kinase was CDK1/cyclin B, and not another CDK complex, was indicated by the temporal and quantitative characteristics of its activation, which closely matched that of CDK1/cyclin B, both during mitosis and mitotic arrest (Fig. 3, 4, 6, 8). In turn, the characteristics of mitotic and MTI-induced Bcl-xL and Bcl-2 phosphorylation closely matched that of CDK1/cyclin B activity, and did not correlate with activation of other CDK complexes including CDK1/cyclin A. Second, validated CDK inhibitors inhibited both mitotic and MTI-induced Bcl-xL/Bcl-2 phosphorylation. Importantly, the CDK inhibitors demonstrated selectivity, as they did not directly inhibit phosphorylation of non-CDK substrates such as histone H3, and further, other kinase inhibitors, including the JNK inhibitor SP600125 (9) and the aurora kinase inhibitor ZM447439 (Fig. S5), had no effect on MTI-induced Bcl-xL/Bcl-2 phosphorylation. In addition, vinblastine induced similar levels of Bcl-xL phosphorylation in both $CDK2^{+/+}$ and $CDK2^{-/-}$ MEFs. Finally, both FL62 and full-length Bcl-xL acted as substrates for purified CDK1, with the latter specifically phosphorylated on the physiologically relevant site, Ser-62, suggesting that CDK1 directly phosphorylates these anti-apoptotic proteins. More recent work from our laboratory has indicated that the anti-apoptotic Bcl-2 member Mcl-1 also undergoes CDK1-mediated phosphorylation upon MTI treatment, which results in Mcl-1 degradation (R. Chu and T.C. Chambers, unpublished data). Thus, CDK1 may be involved in inactivation of all major Bcl-2 family anti-apoptotic proteins during mitotic arrest-induced apoptosis.

This conclusion contrasts with previous reports which have suggested that JNK is responsible for MTI-mediated Bcl-xL or Bcl-2 phosphorylation (2, 11, 36). However, data implicating JNK may be subject to misinterpretation because

JNK inhibitors cause cell cycle delay. In carefully controlled experiments using synchronized cells, we have shown that inhibition of JNK profoundly delays the onset of MTI-induced mitotic block and the corresponding Bcl-xL/Bcl-2 phosphorylation that occurs (9). Thus, co-administration of both a microtubule inhibitor and a JNK inhibition incorrectly gives the appearance of inhibition of Bcl-x/Bcl-2 phosphorylation, when what is actually being observed is delay of phosphorylation. Indeed, validated inhibition of JNK has no effect on the extent of phosphorylation of these proteins (9). In support of this, JNK failed to phosphorylate the peptide substrate FL62 derived from the known *in vivo* site of phosphorylation in Bcl-xL, and FL62 kinase was clearly distinct from JNK isozymes based on chromatographic (Fig. S2) and Cks-1 interaction (Fig. 5) properties. Thus, despite the fact that JNK is strongly activated by MTIs and the sites of phosphorylation are proline-directed, the evidence presented here argues against JNK being responsible for MTI-induced phosphorylation of these proteins.

A previous report showed that the CDK inhibitor flavopiridol inhibited Taxol-induced Bcl-2 phosphorylation (24). Because cells were co-treated with Taxol and flavopiridol, it remained unclear whether the inhibitory effect of flavopiridol was indirectly a consequence of cell cycle suppression. We reported previously that the CDK inhibitor roscovitine failed to appreciably inhibit vinblastine-induced Bcl-xL/Bcl-2 phosphorylation (9). In that study, roscovitine was added to vinblastine-treated synchronized KB-3 cells for 2 h at 12 h post-release. Entirely consistent with those results, we found in this study that if roscovitine was added late at 12-14 h, when phosphorylation had nearly reached a peak, it did not display strong inhibitory activity (Fig. 7B). Roscovitine was most effective when added at earlier time-points, corresponding to the rise in Bcl-xL/Bcl-2 phosphorylation (Fig. 7B and 7D). Indeed, the experimental design shown in Fig. 7A, with multiple inhibitors used at optimal concentration at several intervals, was critical in guiding appropriate conditions for timely CDK1 inhibition, which in turn enabled the generation of more conclusive results.

Both Bcl-xL and Bcl-2 are subject to partial and transient CDK1-mediated phosphorylation during normal mitotic progression (Fig. 4, 8). While mitotic Bcl-2 phosphorylation has been described in several other cell lines (12, 28), the data presented here are the first to show, to our knowledge, mitotic Bcl-xL phosphorylation. The fact that these proteins undergo phosphorylation during normal mitosis may explain why microtubule inhibitors are unique among apoptotic stimuli in promoting phosphorylation. By treating mitotic cells with MG132 and blocking mitotic exit, Bcl-xL/Bcl-2 phosphorylation was dramatically altered, from transient and incomplete to sustained and complete, approaching levels seen in MTI-treated cells (Fig. 8B). These results provide evidence that partial phosphorylation during mitosis is a direct

consequence of the transient nature of CDK1 activation, with loss of CDK1 activity at mitotic exit representing a kinetic limitation on the extent of phosphorylation. Clearly, the low level of phosphorylation that is rapidly reversed as cells reenter G1 phase is compatible with continued cell survival, whereas the high level of phosphorylation through sustained CDK1 activation during mitotic arrest, lasting 16-20 h (9), is associated with an apoptotic outcome. Based on these observations, it is tempting to speculate that the degree of phosphorylation of Bcl-xL and Bcl-2 may be part of a surveillance mechanism which acts as a read-out for the duration of CDK1 activity. Thus, if CDK1 is active transiently, phosphorylation of Bcl-xL and Bcl-2 necessarily fails to reach a critical threshold, whereas if the kinase is active for too long, the threshold is breached, driving phosphorylation beyond a level compatible with cell survival, causing inactivation of anti-apoptotic function and eventual apoptosis. Such a regulatory system, with different fates stemming from the duration of kinase activation, is not without precedent. JNK, for example, has been shown to have either pro-survival or pro-apoptotic properties depending on whether the enzyme is active transiently or in a sustained manner (7). ERK is another example where its sustained activation leads to S phase entry of fibroblasts or differentiation of PC12 cells, whereas transient ERK activation fails to elicit these effects (18). The transcription factor c-Fos has been shown to act as a sensor for ERK signal duration (21). Our results suggest the novel possibility that Bcl-xL and Bcl-2 act as sensors during mitosis for interpretation of CDK1 signal duration.

The role of CDK1 in M-phase progression is well established, but the role of prolonged CDK1 activity occurring in response to sustained activation of the spindle checkpoint is more controversial (5). The results of certain studies suggest that sustained CDK1 activity plays a pro-apoptotic role. For example, CDK1 inhibitors have been shown to block Taxol-induced cell death in several cell systems (6, 29, 38). Because studies with phospho-defective mutants of Bcl-xL and Bcl-2 have consistently suggested that phosphorylation inactivates their anti-apoptotic function (33, 36), our results are consistent with sustained CDK1 activity acting in a pro-apoptotic manner in this context. In support of this possibility, apoptosis induced by non-degradable cyclin B1 was strongly suppressed by co-transfection with phospho-defective Bcl-xL, but was not suppressed by phospho-mimic Bcl-xL (Fig. 11). Thus, Bcl-xL acts as a key substrate for pro-apoptotic CDK1 signaling. However, a cytoprotective role for CDK1 during mitotic arrest, through phosphorylation of survivin (23) or caspase-9 (1), has also been reported. Survivin and caspase-9 operate at the most distal stage of intrinsic apoptosis, whereas Bcl-2 proteins act upstream as regulators. Taken together, the data suggest the intriguing possibility that CDK1 acts as a positive regulator of the preparatory phase of mitotic arrest-induced apoptosis, but as a negative

regulator of the execution phase. The existence of such opposing mechanisms may help explain the differing outcomes produced when CDK inhibitors and MTIs are combined (5).

In conclusion, we have provided strong experimental evidence that CDK1/cyclin B is responsible for mitotic and MTI-induced Bcl-xL and Bcl-2 phosphorylation. The mechanism invoked by these studies, with sustained CDK1 activity catalyzing direct phosphorylation of anti-apoptotic Bcl-2 proteins, provides a functional link coupling mitotic arrest and apoptosis. Further, we propose that these key proteins act as sensors for interpretation of CDK1 signal duration.

ACKNOWLEDGEMENTS

We thank D.R. Green for kindly providing pET29b-BclxL-ΔC plasmid, P. Kaldis for kindly providing mouse embryonic fibroblasts, J. Pines and T.A. Potapova for kindly providing cyclin B1-GFP plasmids, and G. Baldini, S. Mackintosh, R. Kurten, P. Price and G. Gorbsky for helpful discussions and technical assistance. This work was supported by Public Health Service grant CA-109821 from the National Cancer Institute (T.C.C.), by pilot study funds from the UAMS College of Medicine Research Council (T.C.C.), by the Department of Defense Breast Cancer Program Predoctoral Fellowship Award No. BC083287 (D.T.T.), and by an American Cancer Society, Illinois Division, Postdoctoral Fellowship (M.U.). Any opinions, findings, and conclusions or recommendations expressed in this publication are those of the author(s) and do not necessarily reflect the views of the Department of Defense Breast Cancer Program.

1. **Allan, L. A. and P. R. Clarke**. 2007. Phosphorylation of caspase-9 by CDK1/cyclin B1 protects mitotic cells against apoptosis. Mol. Cell **26**:301-310.

2. **Basu, A. and S. Haldar**. 2003. Identification of a novel Bcl-xL phosphorylation site regulating the sensitivity of taxol- or 2-methoxyestradiol-induced apoptosis. FEBS Lett. **538**:41-47.

3. **Blagosklonny, M. V., P. Giannakakou, W. S. El-Deiry, D. G. Kingston, P. I. Higgs, L. Neckers, and T. Fojo**. 1997. Raf-1/bcl-2 phosphorylation: a step from microtubule damage to cell death. Cancer Res. **57**:130-135.

4. **Calastretti, A., A. Bevilacqua, C. Ceriani, S. Vigano, P. Zancai, S. Capaccioli, and A. Nicolin**. 2001. Damaged microtubules can inactivate BCL-2 by means of the mTOR kinase. Oncogene **20**:6172-6180.

5. **Castedo, M., J. L. Perfettini, T. Roumier, and G. Kroemer**. 2002. Cyclin-dependent kinase-1: linking apoptosis to cell cycle and mitotic catastrophe. Cell Death. Differ. **9**:1287-1293.

6. **Chan, Y. W., H. T. Ma, W. Wong, C. C. Ho, K. F. On, and R. Y. Poon**. 2008. CDK1 inhibitors antagonize the immediate apoptosis triggered by spindle disruption but promote apoptosis following the subsequent rereplication and abnormal mitosis. Cell Cycle **7**:1449-1461.

7. **Davis, R. J.** 2000. Signal transduction by the JNK group of MAP kinases. Cell **103**:239-252.

8. **Desagher, S., A. Osen-Sand, A. Nichols, R. Eskes, S. Montessuit, S. Lauper, K. Maundrell, B. Antonsson, and J. C. Martinou**. 1999. Bid-induced conformational change of Bax is responsible for mitochondrial cytochrome c release during apoptosis. J. Cell Biol. **144**:891-901.

9. **Du, L., C. S. Lyle, and T. C. Chambers**. 2005. Characterization of vinblastine-induced Bcl-xL and Bcl-2 phosphorylation: evidence for a novel protein kinase and a coordinated phosphorylation/dephosphorylation cycle associated with apoptosis induction. Oncogene **24**:107-117.

10. **Fan, M., L. Du, A. A. Stone, K. M. Gilbert, and T. C. Chambers**. 2000. Modulation of mitogen-activated protein kinases and phosphorylation of Bcl-2 by vinblastine represent persistent forms of normal fluctuations at G2-M. Cancer Res. **60**:6403-6407.

11. **Fan, M., M. Goodwin, T. Vu, C. Brantley-Finley, W. A. Gaarde, and T. C. Chambers**. 2000. Vinblastine-induced phosphorylation of Bcl-2 and Bcl-xL is mediated by JNK and occurs in parallel with inactivation of the Raf-1/MEK/ERK cascade. J. Biol. Chem. **275**:29980-29985.

12. **Furukawa, Y., S. Iwase, J. Kikuchi, Y. Terui, M. Nakamura, H. Yamada, Y. Kano, and M. Matsuda**. 2000. Phosphorylation of Bcl-2 protein by CDC2 kinase during G2/M phases and its role in cell cycle regulation. J. Biol. Chem. **275**:21661-21667.

13. **Haldar, S., N. Jena, and C. M. Croce**. 1995. Inactivation of Bcl-2 by phosphorylation. Proc. Natl. Acad. Sci. U. S. A **92**:4507-4511.

14. **Harper, J. W.** 2001. Protein destruction: adapting roles for Cks proteins. Curr. Biol. **11**:R431-R435.

15. **Hsu, J. Y., Z. W. Sun, X. Li, M. Reuben, K. Tatchell, D. K. Bishop, J. M. Grushcow, C. J. Brame, J. A. Caldwell, D. F. Hunt, R. Lin, M. M. Smith, and C. D. Allis**. 2000. Mitotic phosphorylation of histone H3 is governed by Ipl1/aurora kinase and Glc7/PP1 phosphatase in budding yeast and nematodes. Cell **102**:279-291.

16. **Kastan, M. B. and J. Bartek**. 2004. Cell-cycle checkpoints and cancer. Nature **432**:316-323.

17. **Letai, A. G.** 2008. Diagnosing and exploiting cancer's addiction to blocks in apoptosis. Nat. Rev. Cancer **8**:121-132.

18. **Marshall, C. J.** 1995. Specificity of receptor tyrosine kinase signaling: transient versus sustained extracellular signal-regulated kinase activation. Cell **80**:179-185.

19. **Meijer, L., A. Borgne, O. Mulner, J. P. Chong, J. J. Blow, N. Inagaki, M. Inagaki, J. G. Delcros, and J. P. Moulinoux**. 1997. Biochemical and cellular effects of roscovitine, a potent and selective inhibitor of the cyclin-dependent kinases cdc2, cdk2 and cdk5. Eur. J. Biochem. **243**:527-536.

20. **Mollinedo, F. and C. Gajate**. 2003. Microtubules, microtubule-interfering agents and apoptosis. Apoptosis. **8**:413-450.

21. **Murphy, L. O., S. Smith, R. H. Chen, D. C. Fingar, and J. Blenis**. 2002. Molecular interpretation of ERK signal duration by immediate early gene products. Nat. Cell Biol. **4**:556-564.

22. **Musacchio, A. and E. D. Salmon**. 2007. The spindle-assembly checkpoint in space and time. Nat. Rev. Mol. Cell Biol. **8**:379-393.

23. **O'Connor, D. S., N. R. Wall, A. C. Porter, and D. C. Altieri**. 2002. A p34(cdc2) survival checkpoint in cancer. Cancer Cell **2**:43-54.

24. **Pathan, N., C. Aime-Sempe, S. Kitada, S. Haldar, and J. C. Reed**. 2001. Microtubule-targeting drugs induce Bcl-2 phosphorylation and association with Pin1. Neoplasia. **3**:70-79.

25. **Poruchynsky, M. S., E. E. Wang, C. M. Rudin, M. V. Blagosklonny, and T. Fojo**. 1998. Bcl-xL is phosphorylated in malignant cells following microtubule disruption. Cancer Res **58**:3331-3338.

26. **Rieder, C. L. and H. Maiato**. 2004. Stuck in division or passing through: what happens when cells cannot satisfy the spindle assembly checkpoint. Dev. Cell **7**:637-651.

27. **Rosania, G. R., J. Merlie, Jr., N. Gray, Y. T. Chang, P. G. Schultz, and R. Heald**. 1999. A cyclin-dependent kinase inhibitor inducing cancer cell differentiation: biochemical identification using Xenopus egg extracts. Proc. Natl. Acad. Sci. U. S. A **96**:4797-4802.

28. **Scatena, C. D., Z. A. Stewart, D. Mays, L. J. Tang, C. J. Keefer, S. D. Leach, and J. A. Pietenpol**. 1998. Mitotic phosphorylation of Bcl-2 during normal cell cycle progression and Taxol-induced growth arrest. J. Biol. Chem. **273**:30777-30784.

29. **Shen, S. C., T. S. Huang, S. H. Jee, and M. L. Kuo**. 1998. Taxol-induced p34cdc2 kinase activation and apoptosis inhibited by 12-O-tetradecanoylphorbol-13-acetate in human breast MCF-7 carcinoma cells. Cell Growth Differ. **9**:23-29.

30. **Skoufias, D. A., R. L. Indorato, F. Lacroix, A. Panopoulos, and R. L. Margolis**. 2007. Mitosis persists in the absence of Cdk1 activity when proteolysis or protein phosphatase activity is suppressed. J. Cell Biol. **179**:671-685.

31. **Sorger, P. K., M. Dobles, R. Tournebize, and A. A. Hyman**. 1997. Coupling cell division and cell death to microtubule dynamics. Curr. Opin. Cell Biol. **9**:807-814.

32. **Srivastava, R. K., A. R. Srivastava, S. J. Korsmeyer, M. Nesterova, Y. S. Cho-Chung, and D. L. Longo**. 1998. Involvement of microtubules in the regulation of Bcl2 phosphorylation and apoptosis through cyclic AMP-dependent protein kinase. Mol. Cell Biol. **18**:3509-3517.

33. **Upreti, M., E. N. Galitovskaya, R. Chu, A. J. Tackett, D. T. Terrano, S. Granell, and T. C. Chambers**. 2008. Identification of the major phosphorylation site in Bcl-xL induced by microtubule inhibitors and analysis of its functional significance. J. Biol. Chem. **283**:35517-35525.

34. **Vassilev, L. T., C. Tovar, S. Chen, D. Knezevic, X. Zhao, H. Sun, D. C. Heimbrook, and L. Chen**. 2006. Selective small-molecule inhibitor reveals critical mitotic functions of human CDK1. Proc. Natl. Acad. Sci. U. S. A **103**:10660-10665.

35. **Weaver, B. A. and D. W. Cleveland**. 2005. Decoding the links between mitosis, cancer, and chemotherapy: The mitotic checkpoint, adaptation, and cell death. Cancer Cell **8**:7-12.

36. **Yamamoto, K., H. Ichijo, and S. J. Korsmeyer**. 1999. BCL-2 is phosphorylated and inactivated by an ASK1/Jun N-terminal protein kinase pathway normally activated at G(2)/M. Mol. Cell Biol. **19**:8469-8478.

37. **Youle, R. J. and A. Strasser**. 2008. The BCL-2 protein family: opposing activities that mediate cell death. Nat. Rev. Mol. Cell Biol. **9**:47-59.

38. **Yu, D., T. Jing, B. Liu, J. Yao, M. Tan, T. J. McDonnell, and M. C. Hung**. 1998. Overexpression of ErbB2 blocks Taxol-induced apoptosis by upregulation of p21Cip1, which inhibits p34Cdc2 kinase. Mol. Cell **2**:581-591.

TABLE 1. In vitro phosphorylation of FL62 by CDK1

Assay condition	^{32}P incorporation (cpm)		
	Assay values	Ave	Net (%)
No substrate	24456, 25131	24974	0
Histone H1	644693, 659460, 658373	654175	629382 (100)
FL62	809686, 813972, 802739	808799	784006 (125)

Active CDK1/cyclin A2 complex was incubated alone or with 5 μg histone H1 or 1 μg FL62 in kinase reaction mix for 20 min at 30°C with 1 μM ATP and 1 μCi [γ-^{32}P]ATP. Reactions were conducted in triplicate and ^{32}P incorporation determined by P81 phosphocellulose paper binding assay.

Figure 1. Phosphorylation of a Bcl-xL kinase peptide substrate. A. Sequence of FL62 peptide representing amino acids 58-66 from the flexible loop (FL) of human Bcl-xL with three C-terminal arginines. Ser62 is indicated. **B.** Electrophoretic detection of FL62. The indicated amounts of FL62 in 10 μL were subjected to high resolution 16.5% acrylamide Tris/Tricine SDS-PAGE and visualized by Coomassie staining, as described in Materials and Methods. Molecular mass standards are indicated. **C**. Phosphorylation of FL62. Protein extracts from untreated (Control; left panels) or vinblastine (VBL; right panels) treated KB-3 cells were size separated by FPLC using a Superdex 200 10/300 column. Fractions were incubated without (- peptide) or with (+ peptide) 50 μg of FL62 in the presence of [γ^{32}P]ATP at 30˚C for 20 min. Reaction mixtures were electrophoresed as in panel B, gels were fixed overnight in 5% glutaraldehyde, washed extensively in dH_2O, and exposed to a phosphorimager screen, with each gel subjected to equal exposure. Fraction numbers are indicated at the top of each gel, and the lower and higher molecular weight forms of phosphorylated FL62 are indicated.

Figure 2. Size exclusion chromatography of FL62 kinase. A. Rapid phosphocellulose filter assay of FL62 kinase activity. The FPLC fractions used in the gel-based assay (Fig. 1C) were reassayed using a P81 filter assay. Fractions 19-26 were incubated with (white bars) or without (black bars) 50 μg FL62 peptide in the presence of [γ^{32}P]ATP at 30˚C for 20 min. Reactions were stopped with 20 mM EDTA, acidified with 15% acetic acid, spotted onto P81 filters, washed in 75 mM H_3PO_4, and dried. ^{32}P radioactivity was determined by scintillation counting. Data shown are representative of eight experiments. **B.** FL62 kinase activity in vinblastine- and Taxol-treated cells. KB-3 cells were treated with 30 nM vinblastine (VBL) for 16 h or 48 h, or 30 nM Taxol (TAX) for 16 h, and extracts resolved by FPLC as in Fig. 1C. Net FL62 kinase activity was determined using the P81 filter paper assay as in panel A by subtracting cpm of reactions without FL62 from those with FL62. **C.** Molecular weight estimation of FL62 kinase. Superdex-200 FPLC absorbance profile at 280 nm (▬) and net FL62 kinase activity (– – –) of 16-h vinblastine extract (panel B) are superimposed on the same graph. The elution positions of 200 kDa and 66 kDa molecular weight standards (β-amylase and albumin, respectively) are shown.

Figure 3. Extent of FL62 kinase activity coincides with degree of G2/M arrest. A. FL62 kinase activity in whole cell extracts. KB-3 cells were untreated or treated with 30 or 100 nM vinblastine (VBL) for 16 h and extracts subjected to FL62 kinase assay, peptide-PAGE, and phosphorimage analysis, as in Fig. 1C. The arrow indicates the migration position of phosphorylated FL62. **B.** Quantitative relationship between FL62 kinase activity, G2/M index, and cellular Bcl-xL phosphorylation, induced by vinblastine. KB-3 cells were treated with vinblastine at the indicated concentrations for 16 h and extracts prepared for determination of FL62 kinase activity (*upper graph)* and immunoblotting for the indicated proteins (*lower panels*). FL62 kinase activity was determined by the P81 phosphocellulose assay with ^{32}P incorporation from reactions without FL62 subtracted from reactions with FL62 to calculate net FL62 phosphorylation. Reactions were performed in triplicate and the average values plotted. The dotted line represents cyclin B expression, determined by densitometry from the blot shown in the lower panel, as described in Materials and Methods. The percentage of cells with 4N DNA was determined by propidium iodide staining and flow cytometry, as described in Materials and Methods.

Figure 4. Partial Bcl-xL/Bcl-2 phosphorylation and FL62 kinase activation during normal mitosis. A. FL62 kinase activity during normal mitosis. Extracts were prepared from untreated asynchronous KB-3 cells (Control), KB-3 cells synchronized in mitosis (mitotic) by double thymidine block with harvest 10 h after release, or asynchronous KB-3 cells treated with 30 nM vinblastine for 16 h. Extracts were incubated without or with FL62 in a kinase reaction and analyzed by the P81 filter assay. FL62 kinase specific activity (pmol phosphate incorporated into FL62 per min per mg of cell extract) is shown for each condition. Results represent mean ± S.D. (n = 6). **B.** Phosphorylation of cellular Bcl-xL during normal mitosis. Extracts from untreated, mitotic, or vinblastine-treated cells (from panel A) were subject to immunoblotting for Bcl-xL and cyclin B. GAPDH was used as a loading control. **C.** Bcl-xL phosphorylation dynamics during the normal cell cycle and following vinblastine treatment. KB-3 cells were synchronized by double thymidine block. Cells were left untreated (Control) or treated with 30 nM vinblastine 1 h after release, and harvested at the indicated times after release. Extracts were subjected to immunoblotting for Bcl-xL, Bcl-2, cyclin B, cyclin A, or GAPDH, as indicated. Phosphorylated Bcl-xL is indicated by an arrow in vinblastine samples and by an arrowhead in control samples (9-12 h time points).

Figure 5. Identification of FL62 kinase as a CDK. A whole cell extract of KB-3 cells treated with vinblastine (30 nM, 16 h) was incubated with Cks-1 conjugated agarose beads. **A.** The original extract and that depleted with Cks-1 were incubated with FL62 (10 μg) or H1 histone (1 μg) for 20 min at 30°C in a kinase reaction containing 10 μM ATP and 1

μCi [γ^{32}P]ATP, and phosphorylation was determined using the P81 filter paper assay. Phosphorylation in the absence of substrate was subtracted. Data shown are mean ± S.D. (n = 3). **B.** The whole cell extract (WCE), as well as the supernatant (S) and the pellet (P) from the Cks-1 pull-down (Cks-1 PD), (15% of the total sample in each case) were immunoblotted for the indicated proteins.

Figure 6. Phosphorylation of FL62 by immunoprecipitated CDK1/cyclin B. A. Extracts were prepared from untreated asynchronous KB-3 cells (control), untreated synchronized cells harvested 10 h after release (mitotic), and asynchronous cells treated with 30 nM vinblastine for 16h (VBL). Cyclin B1 was immunoprecipitated and, after washing, the immunoprecipitates were subjected to FL62 or H1 histone kinase assays, as described in Materials and Methods. Data represent mean ± S.D. (n = 3) with blank (no substrate) values subtracted; p-values are indicated. **B.** Whole cell extracts (WCE) and immunoprecipitates were immunoblotted for CDK1.

Figure 7. Multiple CDK inhibitors inhibit vinblastine-induced Bcl-xL/Bcl-2 phosphorylation. A. Experimental design. The timing of events for cell synchrony by double thymidine block and cell cycle-specific timing of CDK1 inhibition following vinblastine treatment are shown. Lane numbers refer to panel B. **B.** CDK inhibitors block Bcl-xL/Bcl-2 phosphorylation during mitotic arrest. KB-3 cells were synchronized at the G1/S boundary by double thymidine block and treated with 30 nM vinblastine (VBL) 1 h after release. Cells were harvested at 10 h, 11 h, 12 h, and 14 h after release or treated with 25 μM R-roscovitine (Ros), 10 μM purvalanol A (PA), 10 μM RO3306 (RO), or DMSO vehicle (Veh) for 2 h during the 10-12 h, 11-13 h, and 12-14 h time periods after release. An untreated dish from cells harvested immediately after release from the double thymidine block (Con, 0 h) was included as a control. Arrows indicate phosphorylated forms of Bcl-xL, Bcl-2, or phospho-H1 histone. Whole cell extracts were prepared and immunoblotted for the indicated proteins. GAPDH was used as a loading control. **C.** CDK inhibitors maintain inhibition of Bcl-xL phosphorylation when the proteasome is inhibited. KB-3 cells were synchronized at the G1/S boundary by double

thymidine block and treated with 30 nM vinblastine (VBL) 1 h after release. Cells were harvested 11 h after release or incubated for 2 h (i.e. 11-13 h after release) with 25 μM R-roscovitine (Ros), 10 μM purvalanol A (PA), 10 μM RO3306 (RO) or DMSO (Veh) in the presence or absence of the proteasome inhibitor MG132 (20 μM). MG132 was added 20 min prior to the addition of the CDK inhibitors. Immunoblotting for the indicated proteins was performed. Arrows indicate phosphorylated (p) forms. **D.** CDK inhibitors PA and RO block Bcl-xL phosphorylation at concentrations that do not cause mitotic slippage. KB-3 cells were synchronized at the G1/S boundary by double thymidine block and treated with 30 nM vinblastine (VBL) 1 h after release. Cells were harvested 11 h after release or incubated for 2 h (i.e. 11-13 h after release) with 25 μM R-roscovitine (Ros), 1 μM purvalanol A (PA), 1 μM RO3306 (RO) or DMSO vehicle (Veh). Immunoblotting for the indicated proteins was performed. Arrows indicate phosphorylated (p) forms.

Figure 8. CDK inhibitors inhibit mitotic Bcl-xL/Bcl-2 phosphorylation which is normally transient but sustained if mitosis is prolonged. A. Inhibition of CDK inhibits mitotic Bcl-xL/Bcl-2 phosphorylation. KB-3 cells were synchronized at the G1/S boundary by double thymidine block and at 7 h after release either harvested or treated for 2 h with 25 μM R-roscovitine (Ros), 1 μM purvalanol A (PA), 1 μM RO3306 (RO), or DMSO vehicle (Veh). Whole cell extracts were prepared and immunoblotted for the indicated proteins. Arrows indicate phosphorylated (p) forms of Bcl-xL or Bcl-2. GAPDH was used as a loading control. **B.** Prolonging mitosis without microtubule inhibition leads to sustained Bcl-xL/Bcl-2 phosphorylation. KB-3 cells were synchronized at the G1/S boundary by double thymidine block and released into complete medium. Two flasks of cells were untreated and harvested at 1 h and 10 h post-release as controls. Other flasks of cells were treated with DMSO vehicle (Veh) or MG132 (20 μM) at 10 h post-release and harvested at the indicated time points following release. Whole cell extracts were prepared and immunoblotted for the indicated proteins. One flask of synchronized cells was treated with 30 nM vinblastine (VBL) for 24 h as a positive control for sustained mitotic arrest. Arrows indicate phosphorylated (p) forms of Bcl-xL or Bcl-2. GAPDH was used as a loading control

Figure 9. CDK1 phosphorylates full-length Bcl-xL on Ser-62 *in vitro*. A. CDK1 phosphorylation of full-length Bcl-xL. HisBclxL-ΔC (5 μg) was incubated with 0-320 ng of purified, active CDK1/cyclin A2 in a kinase reaction with

[γ^{32}P]ATP and subjected to SDS-PAGE, Coomassie Blue staining, and phosphorimager analysis. HisBclxL-ΔC is indicated by the arrows. **B.** Phosphosite mapping of HisBclxL phosphorylated by CDK1. HisBclxL-ΔC (5 μg) was incubated without or with CDK1/cyclin A2 (100 ng) for 5 h at 30˚C in a kinase reaction with non-radioactive ATP. Reactions were subjected to SDS-PAGE and Coomassie staining. HisBclxL-ΔC is indicated by an arrow and molecular weight markers are shown. **C.** CDK1 phosphorylates Bcl-xL on Ser62. The bands from each lane in panel B were excised, digested with protease AspN, and peptides analyzed by electrospray-interface LTQ XL-Orbitrap mass spectrometry, as described in Materials and Methods. The covered sequence (51%) is underlined and bold. Ser62 is shaded by a grey box. A representative spectrum from HisBclxL-ΔC incubated with CDK1 shows the single detected phosphopeptide, DpSPAVNGATGHSSL, on Ser62 (S+80, indicating a molecular mass gain of 80 Da). Phosphorylation was not detected in HisBclxL-ΔC from the control reaction. Deamidation of Asn-66 is indicated by the N+1 designation.

Figure 10. FL62 kinase localizes to the mitochondria after vinblastine treatment. A. KB-3 cells were untreated or treated with 30 nM vinblastine (VBL) for 16 h, mitochondrial fractions were prepared by sucrose density centrifugation, and incubated without or with FL62 in a radioactive kinase reaction in duplicate. Reactions were subjected to peptide-PAGE and phosphorimager analysis, with 24 h exposure. The higher and lower molecular weight forms of phosphorylated FL62 are indicated. **B.** FL62 kinase activity in purified mitochondria from vinblastine treated cells. Assays were conducted in triplicate and ^{32}P incorporation determined by the P81 filter assay. Results are shown as mean ± S.D. with p-value. **C.** Cytosolic and mitochondrial molecular markers. Cytosolic and mitochondrial fractions from control (CON) and vinblastine (VBL) samples in panel A were immunoblotted for cytosolic (Caspase-3) and the indicated mitochondrial markers from the oxidative phosphorylation complex (OXPHOS) of enzymes, including ATP Synthase (upper band) and Complex III (lower band). **D.** Subcellular localization of CDK1 by immunoflorescence. KB-3 cells were untreated (Control) or treated with 30 nM vinblastine for 16 h. The cells were co-stained with Mitotracker (Red), polyclonal CDK1 antibody followed by goat anti-mouse secondary antibody conjugated to FITC (green), or DAPI (blue). Arrows indicate mitotic cells with condensed chromosomes. **E.** Subcellular localization of cyclin B. KB-3 cells were untreated (Control) or treated with 30 nM vinblastine for 16 h. The cells were co-stained with Mitotracker (Red), monoclonal cyclin B antibody followed by goat anti-mouse secondary antibody conjugated to FITC (green), or DAPI (blue). Arrows indicate mitotic cells with condensed chromosomes.

Figure 11. Phospho-defective Bcl-xL blocks cell death induced by non-degradable cyclin B1. A. KB-3 cells were transfected with 1 μg plasmid DNA encoding GFP vector, wild-type cyclin B1-GFP, or cyclin B1(R42A)-GFP. *Left*, 48 h post-transfection, cells were subjected to apoptotic cell death ELISA assay (mean ± S.D., n = 6). *Right,* extracts were made and subjected to immunoblotting for cyclin B1 (24 h post-transfection), PARP (48 h post-transfection) or GAPDH. **B.** KB-3 cells were transfected with 1 μg plasmid DNA encoding cyclin B1(R42A)-GFP together with 1 μg plasmid DNA encoding either wild-type (wt), phospho-defective (S62A) or phospho-mimic (S62D) HA-Bcl-xL. *Left*, 48 h post-transfection, cells were subjected to apoptotic cell death ELISA assay (mean ± S.D., n = 6). * $p \leq 0.001$ versus wild-type Bcl-xL; ** $p \leq 0.422$ versus wild-type Bcl-xL. *Right,* extracts were made and subjected to immunoblotting for PARP (48 h post-transfection), HA-tag (48 h post-transfection) or GAPDH.

Figure 1

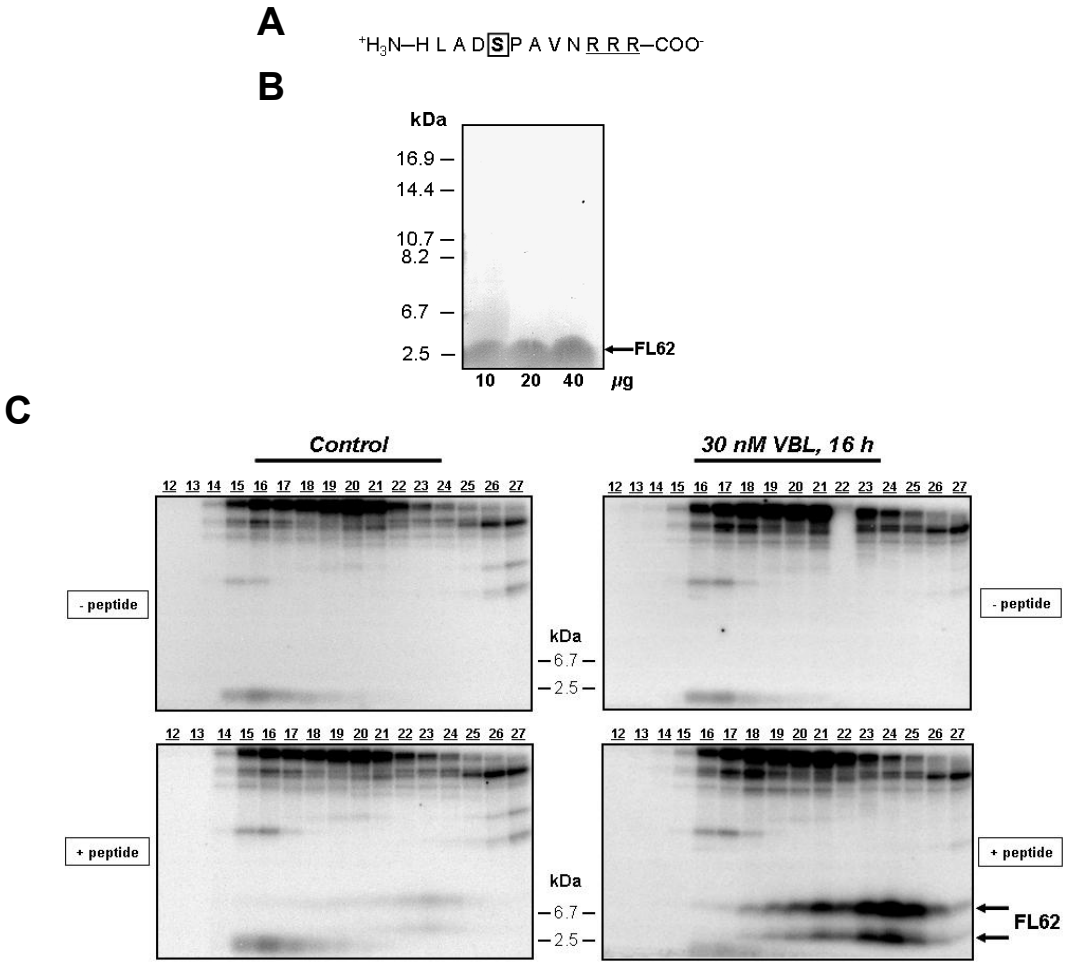
A
+H3N–H L A D S P A V N R R R–COO-
B
kDa
16.9
14.4
10.7
8.2
6.7
2.5
FL62
10 20 40 µg
C
Control
30 nM VBL, 16 h
12 13 14 15 16 17 18 19 20 21 22 23 24 25 26 27
- peptide
+ peptide
kDa
6.7
2.5
FL62

Figure 2

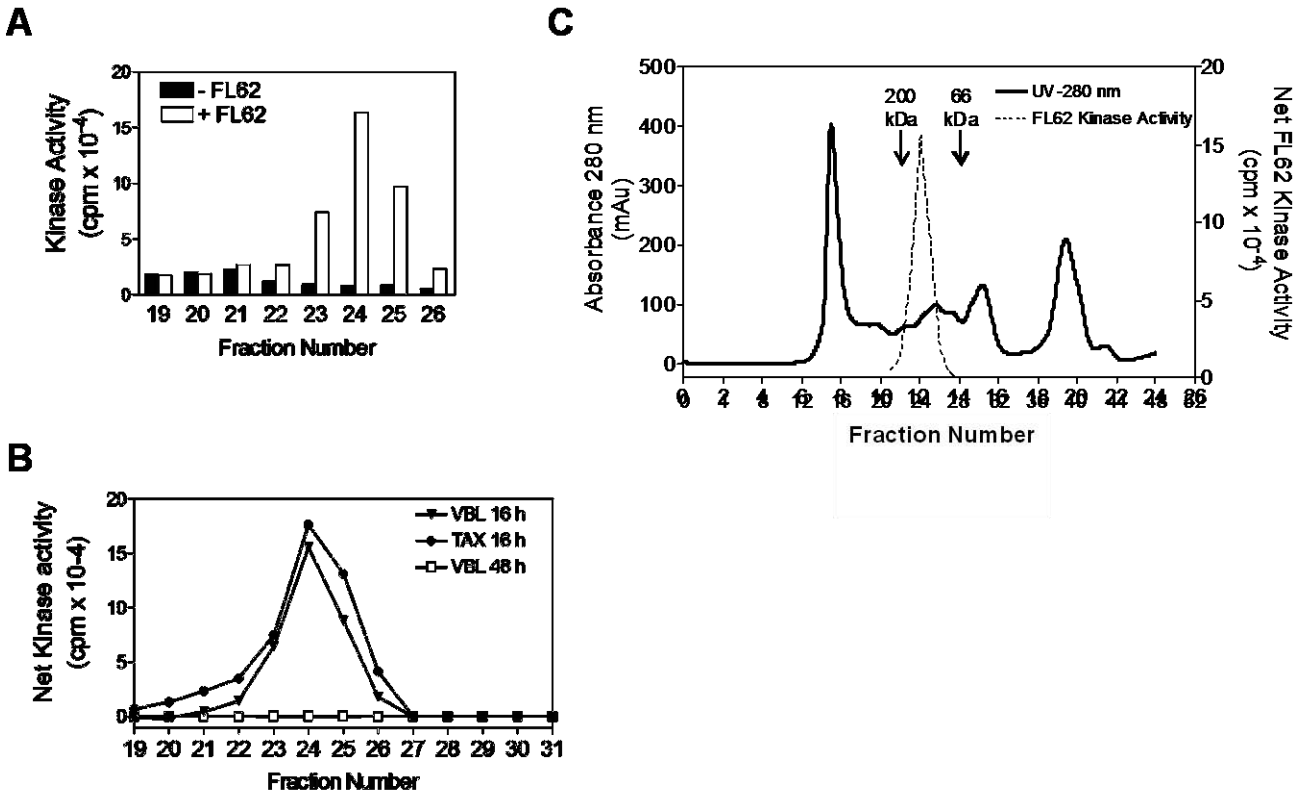
A
- FL62
+ FL62
Kinase Activity (cpm x 10⁻⁴)
Fraction Number
B
VBL 16 h
TAX 16 h
VBL 48 h
Net Kinase activity (cpm x 10-4)
Fraction Number
C
200 kDa
66 kDa
UV-280 nm
FL62 Kinase Activity
Absorbance 280 nm (mAu)
Net FL62 Kinase Activity (cpm x 10⁻⁴)
Fraction Number

Figure 3

A

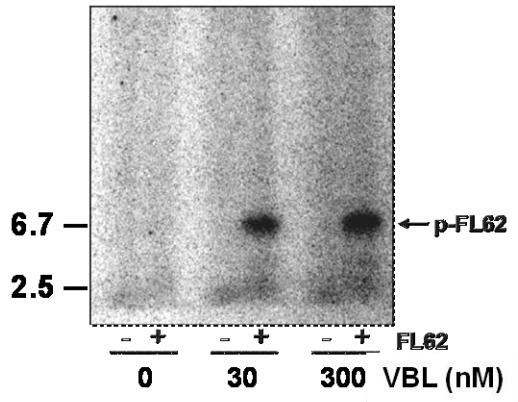
6.7
2.5
p-FL62
- + - + - +
FL62
0 30 300 VBL (nM)

B

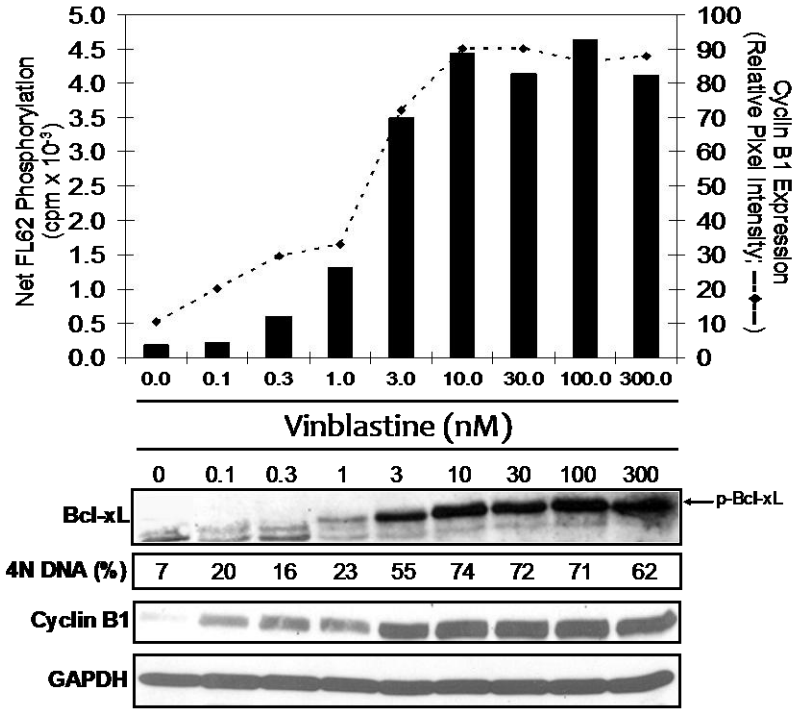
Net FL62 Phosphorylation (cpm x 10-3)
Cyclin B1 Expression (Relative Pixel Intensity; ---◆---)
0.0 0.1 0.3 1.0 3.0 10.0 30.0 100.0 300.0
Vinblastine (nM)
0 0.1 0.3 1 3 10 30 100 300
Bcl-xL
p-Bcl-xL
4N DNA (%)
7 20 16 23 55 74 72 71 62
Cyclin B1
GAPDH

Figure 4

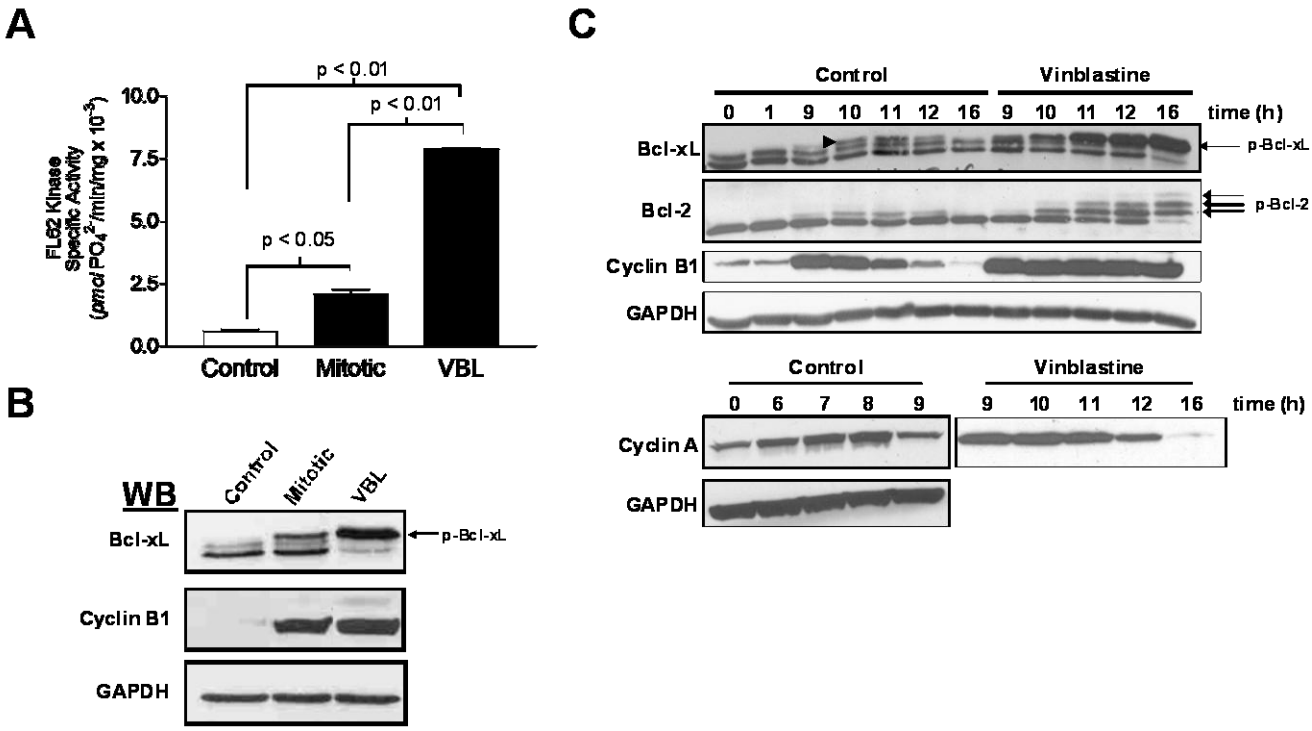
A
p < 0.01
p < 0.01
p < 0.05
FL62 Kinase Specific Activity (pmol PO4 2-/min/mg x 10-3)
10.0
7.5
5.0
2.5
0.0
Control
Mitotic
VBL
B
WB
Control
Mitotic
VBL
Bcl-xL
p-Bcl-xL
Cyclin B1
GAPDH
C
Control
Vinblastine
0 1 9 10 11 12 16 9 10 11 12 16 time (h)
Bcl-xL
p-Bcl-xL
Bcl-2
p-Bcl-2
Cyclin B1
GAPDH
Control
Vinblastine
0 6 7 8 9 9 10 11 12 16 time (h)
Cyclin A
GAPDH

Figure 5

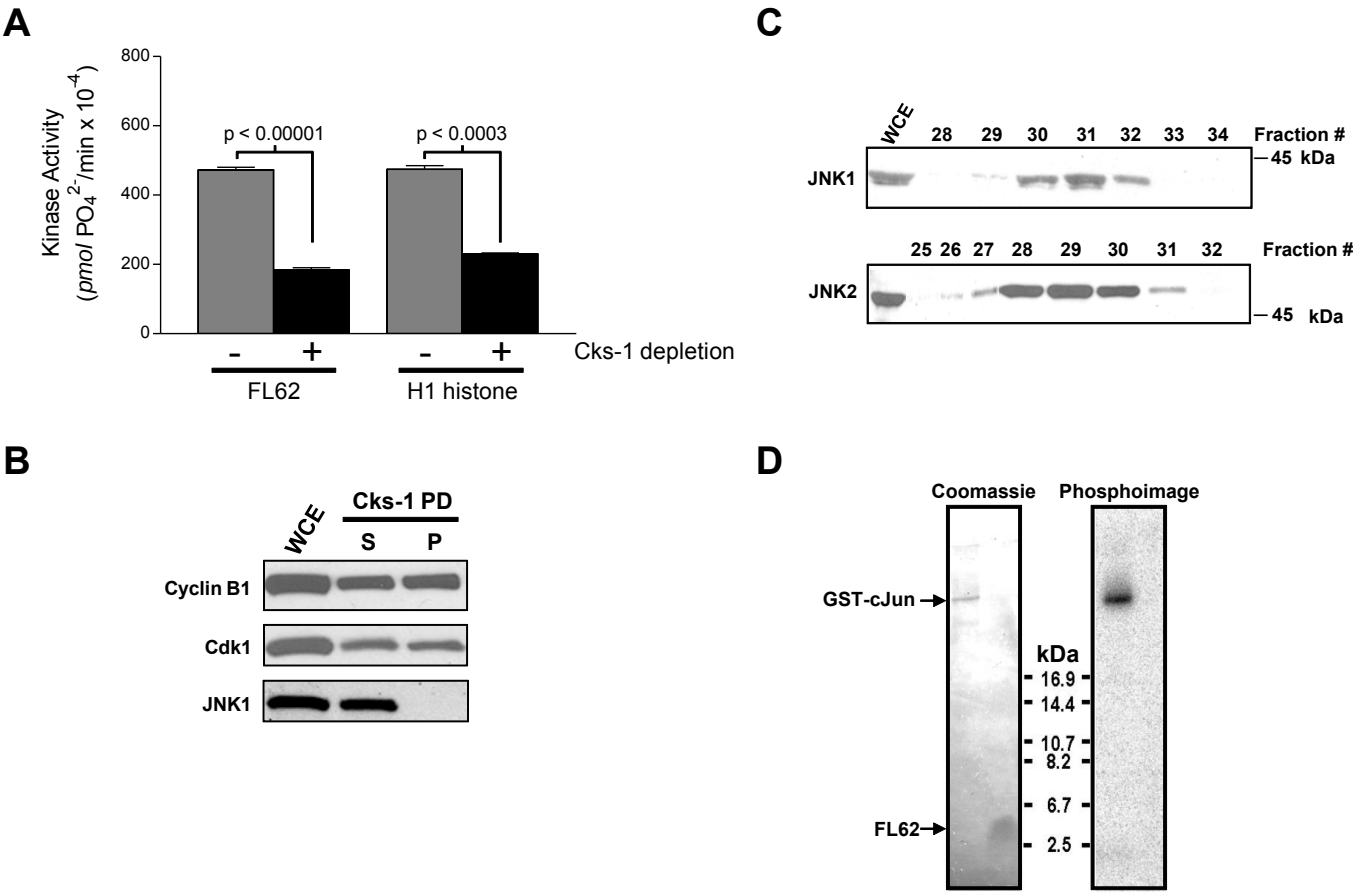
A
Kinase Activity
(pmol PO4 2-/min x 10-4)
800
600
400
200
0
p < 0.00001
p < 0.0003
- + - +
Cks-1 depletion
FL62
H1 histone
C
WCE
28 29 30 31 32 33 34
Fraction #
JNK1
45 kDa
25 26 27 28 29 30 31 32
Fraction #
JNK2
45 kDa
B
WCE
Cks-1 PD
S P
Cyclin B1
Cdk1
JNK1
D
Coomassie
Phosphoimage
GST-cJun
FL62
kDa
16.9
14.4
10.7
8.2
6.7
2.5

Figure 6

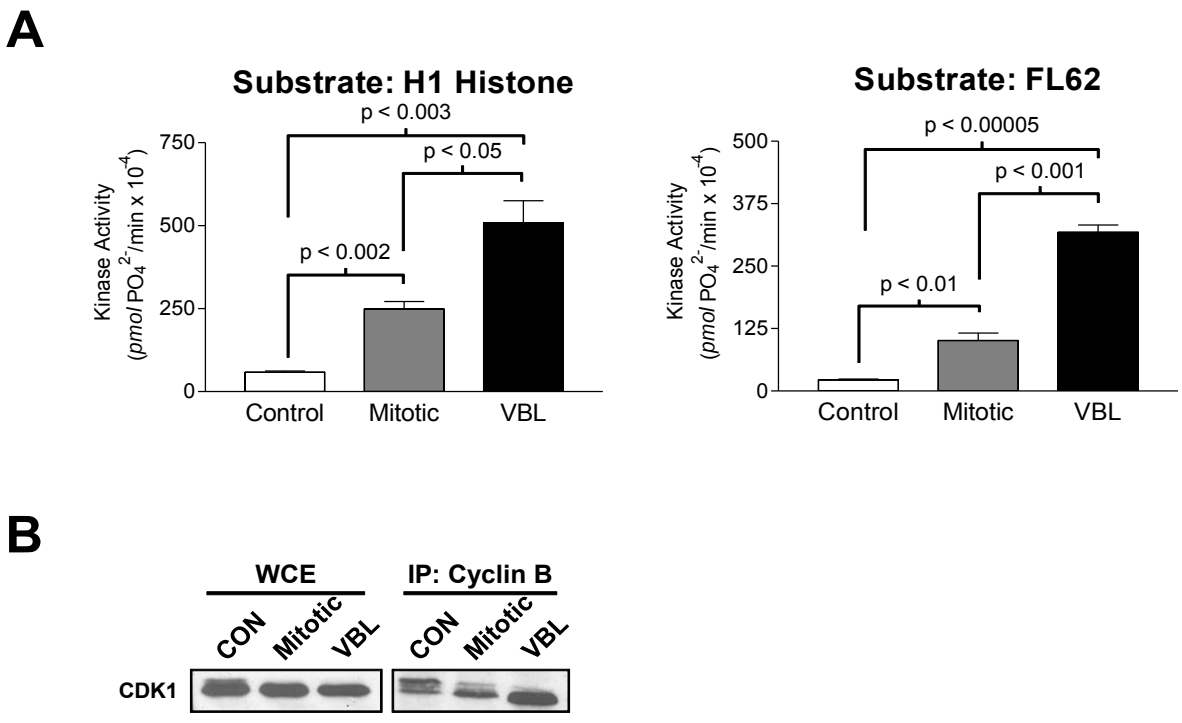
A
Substrate: H1 Histone
p < 0.003
p < 0.05
p < 0.002
Kinase Activity
(pmol PO4 2- /min x 10-4)
750
500
250
0
Control
Mitotic
VBL
Substrate: FL62
p < 0.00005
p < 0.001
p < 0.01
500
375
250
125
0
Control
Mitotic
VBL
B
WCE
IP: Cyclin B
CON
Mitotic
VBL
CON
Mitotic
VBL
CDK1

Figure 7

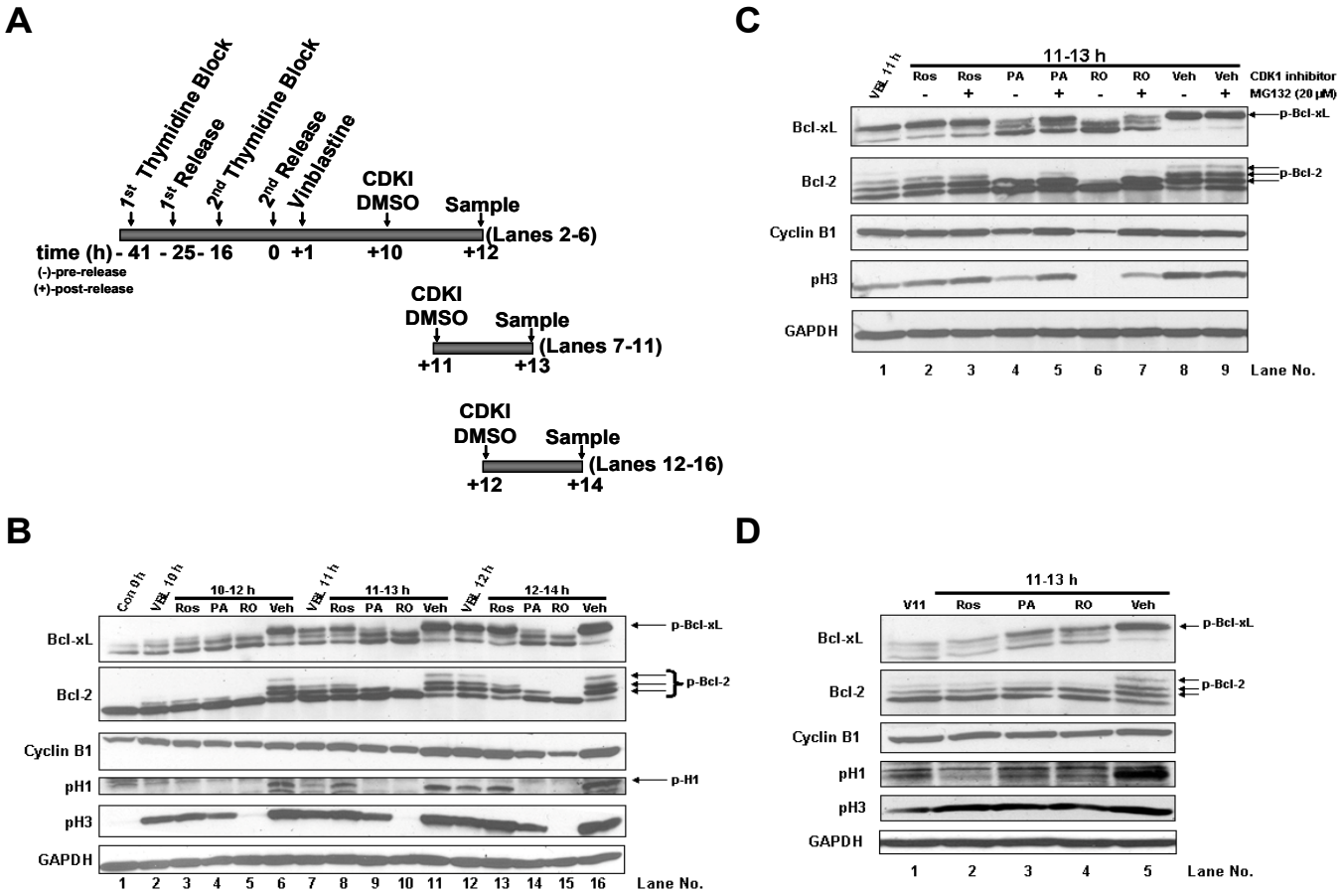
A
1st Thymidine Block
1st Release
2nd Thymidine Block
2nd Release
Vinblastine
CDKI
DMSO
Sample
(Lanes 2-6)
time (h) - 41 - 25 - 16 0 +1 +10 +12
(-)-pre-release
(+)-post-release
CDKI
DMSO
Sample
(Lanes 7-11)
+11 +13
CDKI
DMSO
Sample
(Lanes 12-16)
+12 +14
B
Con 0 h
Veh 10 h
10-12 h
Ros PA RO Veh
Veh 11 h
11-13 h
Ros PA RO Veh
Veh 12 h
12-14 h
Ros PA RO Veh
Bcl-xL
Bcl-2
Cyclin B1
pH1
pH3
GAPDH
p-Bcl-xL
p-Bcl-2
p-H1
1 2 3 4 5 6 7 8 9 10 11 12 13 14 15 16
Lane No.
C
Veh 11 h
11-13 h
Ros Ros PA PA RO RO Veh Veh
CDK1 inhibitor
MG132 (20 μM)
- + - + - + - +
Bcl-xL
Bcl-2
Cyclin B1
pH3
GAPDH
p-Bcl-xL
p-Bcl-2
1 2 3 4 5 6 7 8 9
Lane No.
D
V11
11-13 h
Ros PA RO Veh
Bcl-xL
Bcl-2
Cyclin B1
pH1
pH3
GAPDH
p-Bcl-xL
p-Bcl-2
1 2 3 4 5
Lane No.

Figure 7

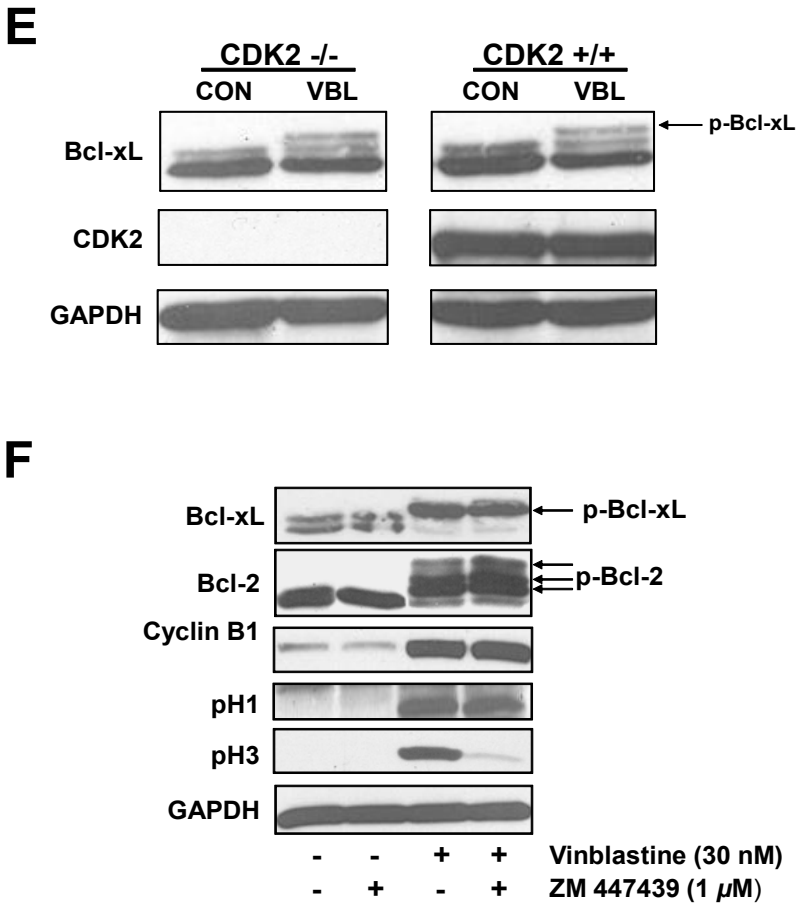
E
CDK2 -/-
CDK2 +/+
CON
VBL
CON
VBL
Bcl-xL
p-Bcl-xL
CDK2
GAPDH
F
Bcl-xL
p-Bcl-xL
Bcl-2
p-Bcl-2
Cyclin B1
pH1
pH3
GAPDH
- - + + Vinblastine (30 nM)
- + - + ZM 447439 (1 μM)

Figure 8

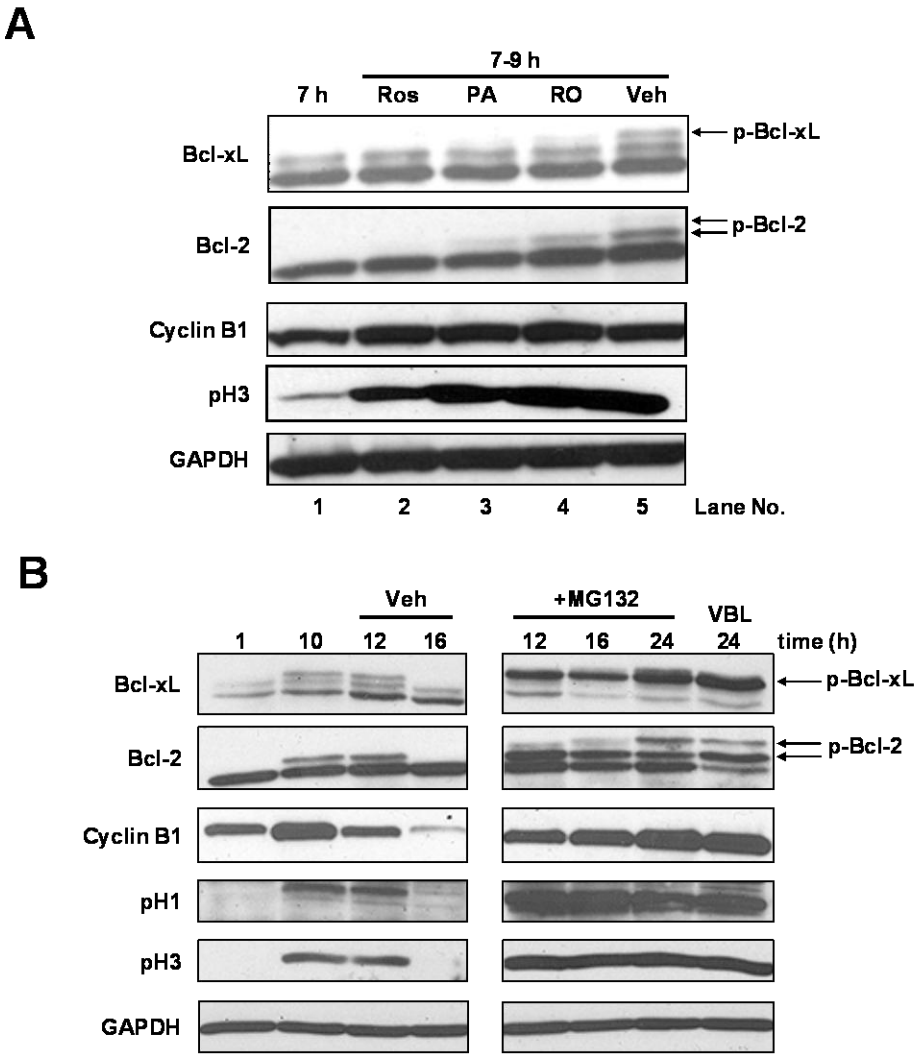
A
7-9 h
7 h
Ros
PA
RO
Veh
Bcl-xL
p-Bcl-xL
Bcl-2
p-Bcl-2
Cyclin B1
pH3
GAPDH
1
2
3
4
5
Lane No.
B
Veh
+MG132
VBL
1
10
12
16
12
16
24
24
time (h)
Bcl-xL
p-Bcl-xL
Bcl-2
p-Bcl-2
Cyclin B1
pH1
pH3
GAPDH

Figure 9

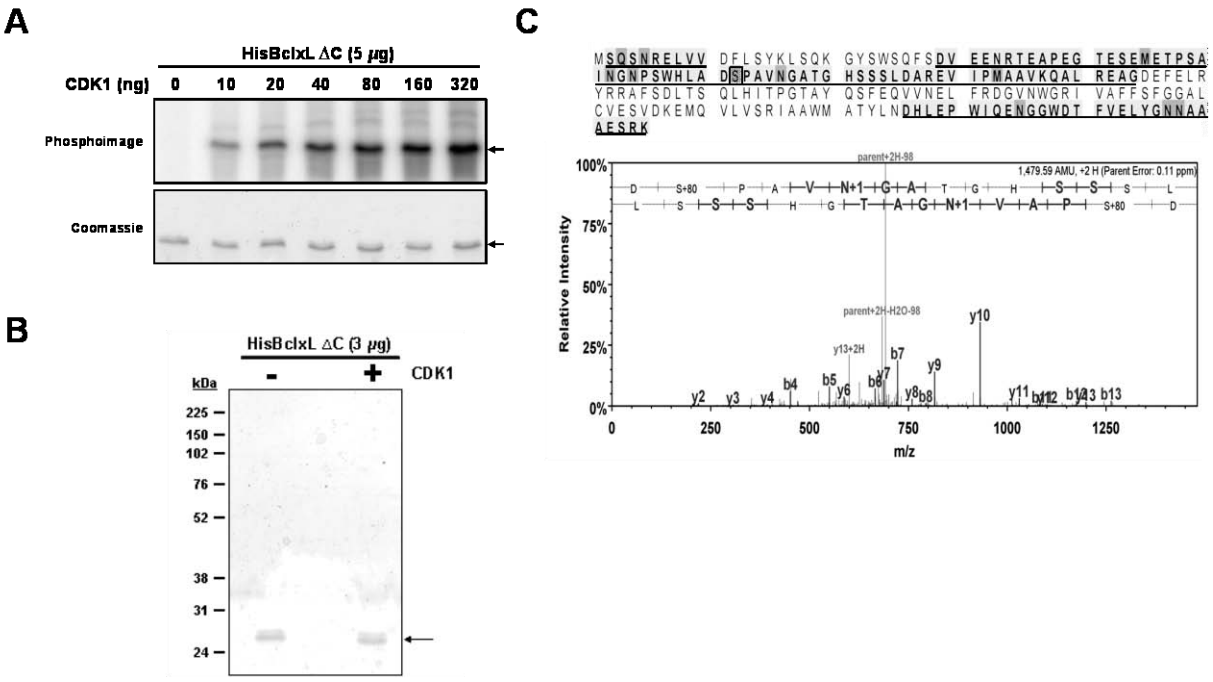
A
HisBclxL ΔC (5 μg)
CDK1 (ng) 0 10 20 40 80 160 320
Phosphoimage
Coomassie
B
HisBclxL ΔC (3 μg)
- +
CDK1
kDa
225
150
102
76
52
38
31
24
C
MSQSNRELVV DFLSYKLSQK GYSWSQFSDV EENRTEAPEG TESEMETPSA
INGNPSWHLA DSPAVNGATG HSSSLDAREV IPMAAVKQAL REAGDEFELR
YRRAFSDLTS QLHITPGTAY QSFEQVVNEL FRDGVNWGRI VAFFSFGGAL
CVESVDKEMQ VLVSRIAAWM ATYLNDHLEP WIQENGGWDT FVELYGNNAA
AESRK
parent+2H-98
1,479.59 AMU, +2 H (Parent Error: 0.11 ppm)
D S+80 P A V N+1 G A T G H S S S L
L S S S H G T A G N+1 V A P S+80 D
Relative Intensity
100%
75%
50%
25%
0%
parent+2H-H2O-98
y13+2H
y10
b7
y9
b5
b4
y6
b6
y7
y8
b8
y2
y3
y4
y11
b12
b13
0
250
500
750
1000
1250
m/z

Figure 10

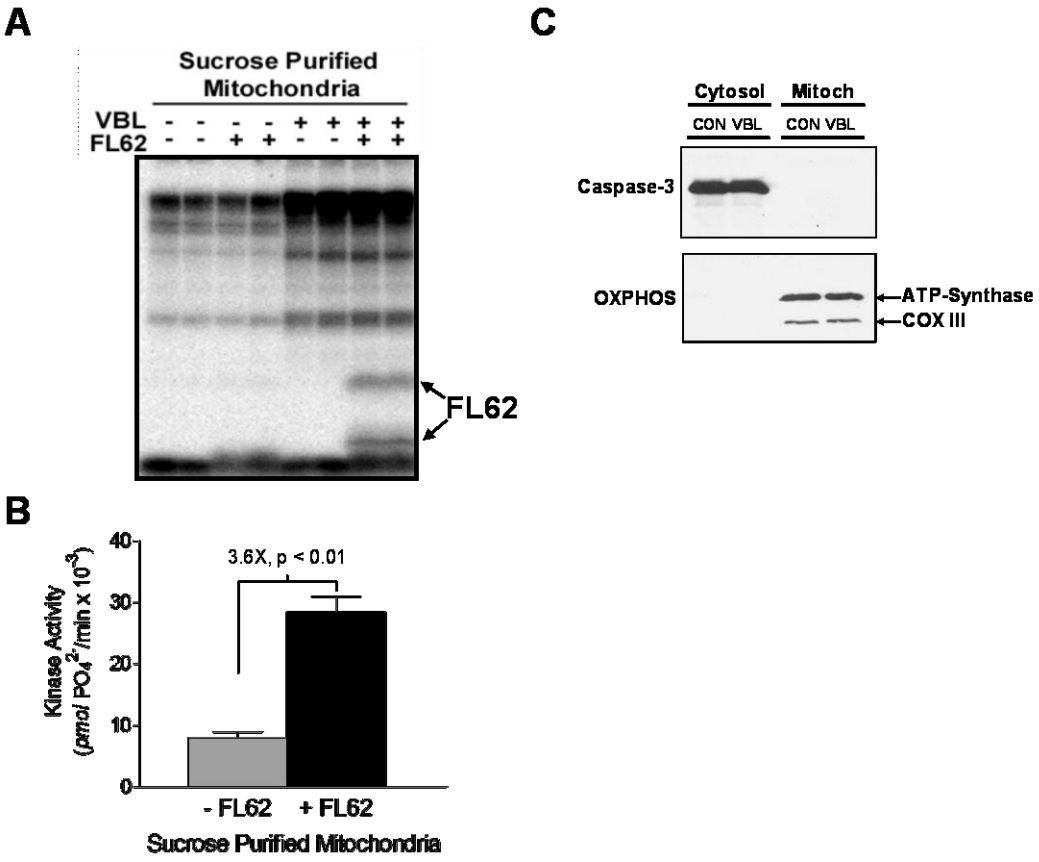
A
Sucrose Purified Mitochondria
VBL - - - - + + + +
FL62 - - + + - - + +
FL62
B
3.6X, p < 0.01
Kinase Activity (pmol PO4 2-/min x 10-3)
40
30
20
10
0
- FL62
+ FL62
Sucrose Purified Mitochondria
C
Cytosol
Mitoch
CON VBL
CON VBL
Caspase-3
OXPHOS
ATP-Synthase
COX III

Figure 10

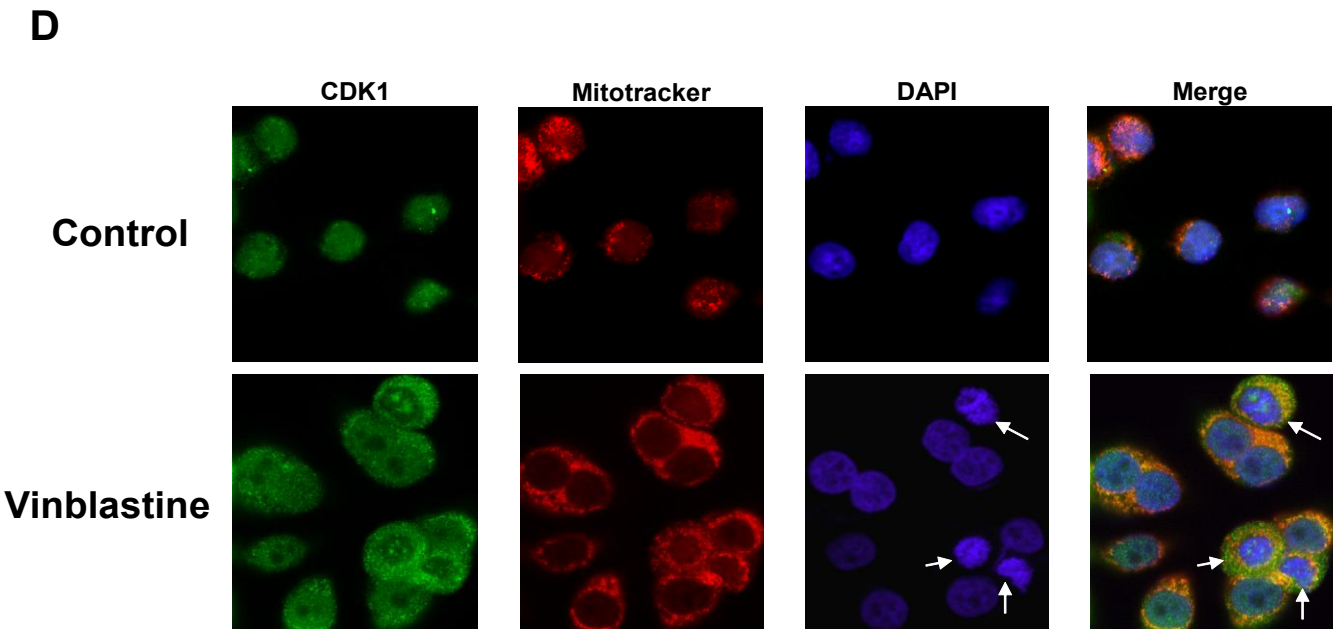

Figure 10

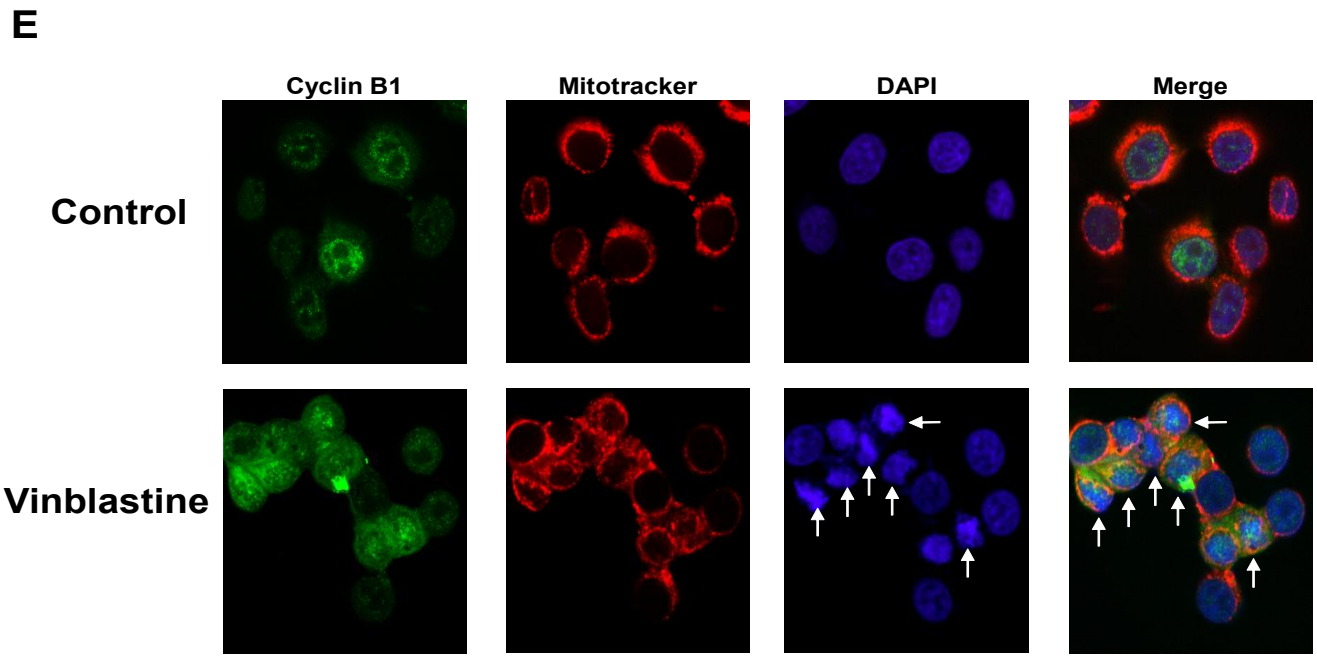

Figure 11

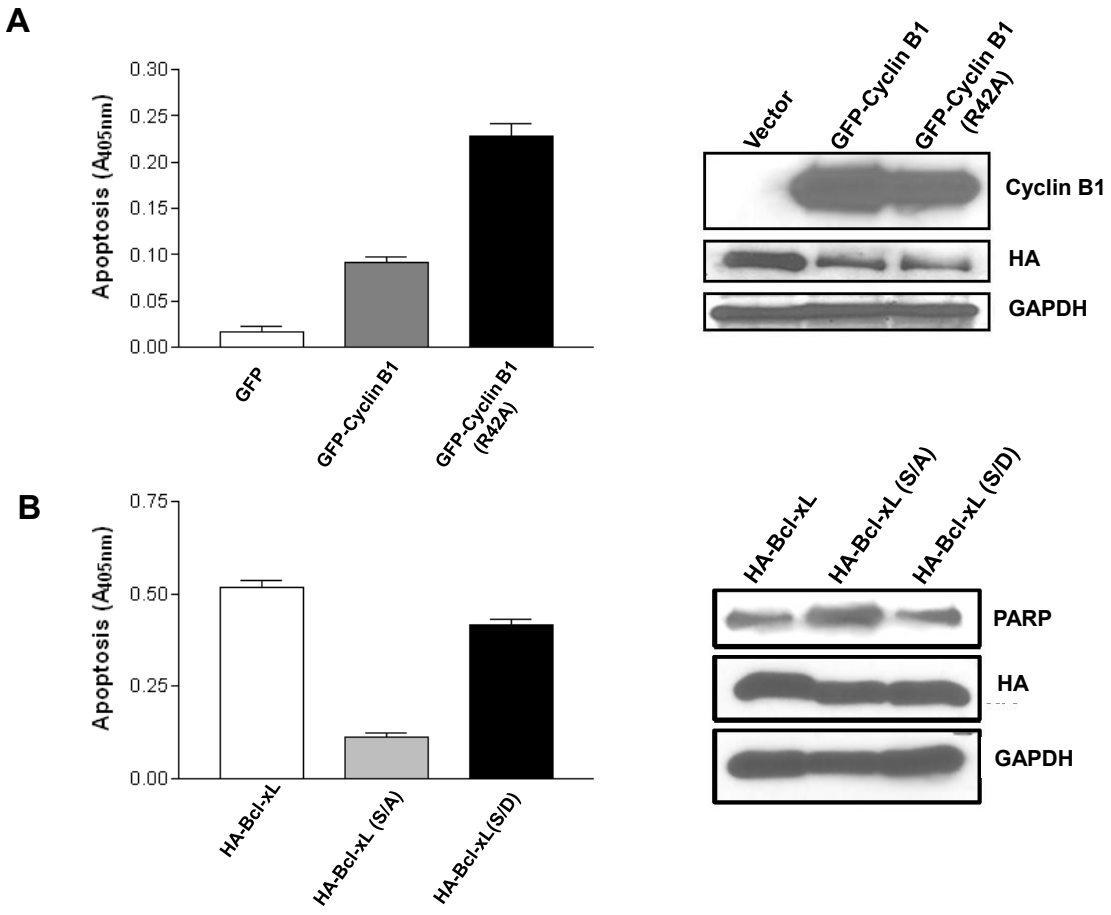
A
Apoptosis (A405nm)
0.30
0.25
0.20
0.15
0.10
0.05
0.00
GFP
GFP-Cyclin B1
GFP-Cyclin B1 (R42A)
Vector
GFP-Cyclin B1
GFP-Cyclin B1 (R42A)
Cyclin B1
HA
GAPDH
B
Apoptosis (A405nm)
0.75
0.50
0.25
0.00
HA-Bcl-xL
HA-Bcl-xL (S/A)
HA-Bcl-xL (S/D)
HA-Bcl-xL
HA-Bcl-xL (S/A)
HA-Bcl-xL (S/D)
PARP
HA
GAPDH